



COLLEGE OF SCIENCE AND TECHNOLOGY
SCHOOL OF SCIENCES
DEPARTMENT OF MATHEMATICS

***ESTIMATION OF SURFACE TEMPERATURES
FROM INTERIOR MEASUREMENTS***

Ngendahayo Jean Pierre

Master of Science
in
Applied Mathematics

2018



COLLEGE OF SCIENCE AND TECHNOLOGY
SCHOOL OF SCIENCES
DEPARTMENT OF MATHEMATICS

***ESTIMATION OF SURFACE TEMPERATURES
FROM INTERIOR MEASUREMENTS***

By
Ngendahayo Jean Pierre

Student number: 217131131

Thesis Submitted in Partial Fulfillment of the Academic Degree of
Master of Science
in
Applied Mathematics
Option of Mathematical Modeling and Scientific Computing

Supervisors: Dr. Fredrik Berntsson; Dr. Japhet Niyobuhungiro

Kigali-Rwanda
April, 2018

Declaration

I, NGENDAHAYO Jean Pierre, hereby declare that this masters thesis titled “*Estimation of Surface Temperatures from Interior Measurements*” is my original work and has never been submitted or presented in any University or Institution of higher learning for academic purposes or otherwise. This was done under supervision of Dr. Fredrik Berntsson¹ and Dr. Japhet Niyobuhungiro².

April 15, 2018

NGENDAHAYO Jean Pierre

¹Linköping University, Sweden

²University of Rwanda-College of Science and Technology, Rwanda

Dedication

*To my family and all peoples who have been inspired me
in science.*

Abstract

The main objective of the thesis is to estimate the surface temperature of a steel slab by solving an inverse heat conduction problem. This problem arises in applications, for example in steel industry, where it is of great importance to be able to control the surface temperature and heating or cooling rates during heat treatment processes in order to achieve good quality of the end products. However, in many industrial applications, the surface itself is inaccessible for direct measurements or locating a measurement device such as a thermocouple on the surface would disturb the measurements so that an incorrect temperature measurement is recorded. In this situation, we are restricted to interior measurements, from which we approximate the surface temperature by solving an inverse heat conduction problem in the region between the surface and a measurement point, because this process is strongly influenced by the time dependent temperature and heat-flux close to the surface.

In this thesis we formulate the problem as an operator equation $Kf = g$, where K is an operator that maps the surface temperature $f(t)$ to the interior measured temperature data $g(t)$, and we need to solve for the unknown surface temperature $f(t)$. However, two main complications arise. Firstly, the operator K is non-linear while most efficient regularization methods are designed for solving linear operator equations. Secondly, due to random noise in measurements, only noisy version g^δ of the exact data g is available in practice, thus solving for f is an *ill-posed problem* in the sense that the solution does not depend continuously on the data. To address these issues, we present in this thesis an approach of rewriting K as a linear operator equation. Also, ill-posedness is investigated and we implement a regularization approach based on Tikhonov method.

Finally, the developed method is applied to a real industrial problem with measured data taken during an industrial steel quenching process. Numerical experiments show that the method works well. We also consider improving the accuracy of the solution by including more measurements, and discuss how making use of the additional data may improve the estimate of the surface temperature as well as improving the stability of the inverse problem.

Keywords and phrases: Inverse heat conduction problem (IHCP), Tikhonov regularization, Steel slab, Industrial steel quenching process, Operator equation.

Acknowledgment

I would like to acknowledge and give thanks in a special way to my supervisors, Dr. Fredrik Berntsson and Dr. Japhet Niyobuhungiro for their commitment, effort, advice, review, encouragement and guidance that made this work fruitful, without them I would not have completed it. And also I would like to take time to thanks Dr. Frderik Berntsson for let his papers about inverse heat conduction problem, especially [12] which include the description about the industrial application presented in this thesis be available and providing the actual measured data from that experiment to be used in this thesis.

I thank my mother, grand brothers, and sisters, for their personal care, financial and moral support during the whole study program.

Finally, I would like to acknowledge the financial support, school fees, I have received from University of Rwanda through the Department of Mathematics. All involved peoples are deeply acknowledged.

CONTENTS

Declaration	i
Dedication	ii
Abstract	iii
Acknowledgment	iv
1. Introduction	1
1.1 Theory of Inverse Heat Conduction Problem	1
1.1.1 Heat conduction	1
1.1.2 Methods of solving IHCP	4
1.1.3 Ill-posedness of IHCP	4
1.2 Background of the problem	5
1.2.1 Statement of the problem	5
1.2.2 Application	6
1.3 Objective	8
1.4 Related works	8
2. Estimation of surface temperature	10
2.1 A Linear operator equation and its properties	11
2.2 Discretization using finite differences	16
2.3 Linear discrete problem	19
2.4 Regularization of the discrete problem	21
2.4.1 Tikhonov regularization	23
2.4.2 Parameter choice rule	26
2.4.3 Numerical experiments	28
2.5 Extension to multiple measurements	31
2.5.1 Numerical experiments	33
3. Temperature estimation on a steel surface	37
3.1 Experimental setup	37
3.2 Data and computational results	38
4. Discussion and conclusion	41
<i>Bibliography</i>	<i>43</i>

1. INTRODUCTION

1.1 Theory of Inverse Heat Conduction Problem

1.1.1 Heat conduction

Consider a thin rod of metal as shown in *Fig.1.1*. When it is heated at the surface *A*, the heat

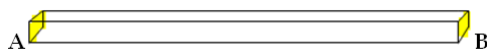


Fig. 1.1: Thin rod of metal

will flow from hottest region to coldest region *B*, i.e from *A* to *B*. In [1] the author postulated the fundamental hypothesis for mathematical theory of heat conduction as follows: *The rate at which heat crosses from the inside to the outside of an isothermal surface per unit area per unit time is equal to*

$$-\kappa \frac{\partial T}{\partial n}, \quad (1.1)$$

where T is the temperature of the surface, κ the thermal conductivity of the substance, and $\partial/\partial n$ denotes differentiation along the outward drawn normal to the surface. As its name indicates the heat equation is used in applications which require the heat conduction, thus it was derived using the theory of heat conduction through the body material which are change of heat quantity in body material, Fourier's law of heat conduction and conservation energy law as summarized here:

Now, let assume that the thin rod has insulated sides and the material has constant density ρ in (kg/m^3) , constant specific heat capacity c_p in (Ws/kgK) , constant cross section S in (m^2) and assume that there is no heat source within the rod and only an external heat source. Heat conduction in this case can be approximated as one-dimensional problem in x -direction with the temperature $T(x, t)$ at length x and at time t . And also in the absence of work done, the change of energy in the body material per unit volume, ΔQ is given as

$$\Delta Q = c_p \Delta M \Delta T = c_p \rho S \Delta x \Delta T. \quad (1.2)$$

We can see that it is directly proportional to the mass M in (kg) of the material and to the increase in temperature ΔT in (K/m) .

A particular case of equation (1.1) is when the isothermal surface is perpendicular to the x -axis, it leads to *Fourier's law of heat conduction* which states that "the rate of heat flowing

into a body through a small surface element on its boundary is proportional to the area of that element and to the outward normal derivative of the temperature at that location in positive direction of x -axis."

$$\dot{Q} = -\kappa \frac{\partial T}{\partial x} \quad (1.3)$$

where \dot{Q} is the density heat flux in (W/m^2) , κ in (W/Km) is the thermal conductivity of the material which depends on temperature and so for x . If T increases as x increases, the rate will be negative and also if T decrease as x increase the rate will be positive.

Therefore, using equations (1.2) and (1.3), and conservation energy law, the following equation (1.4) that describes the physical processes of heat conduction inside the body material where it flows from one position to another in one dimensional was derived and is known as *Heat conduction equation*, [2, 3, 4, 5].

$$\rho c_p \frac{\partial T(x, t)}{\partial t} = \frac{\partial}{\partial x} \left(\kappa \frac{\partial T(x, t)}{\partial x} \right), \quad (1.4)$$

where the *thermal conductivity* κ remains inside of derivative since it depends on x . One can note that when the thermal conductivity κ is constant, the equation (1.4) is reduced to well known heat equation (1.5)

$$\frac{\partial T}{\partial t} = \alpha^2 \frac{\partial^2 T}{\partial x^2} \quad (1.5)$$

with the *thermal diffusivity*, $\alpha^2 = (\kappa/\rho c_p)$.

In [6, 7] it has been shown that the heat equation (1.5) has the following fundamental solution on the whole real line

$$F(x, t) := \begin{cases} \frac{1}{2\alpha\sqrt{\pi t}} \exp\left(-\frac{|x|^2}{4\alpha^2 t}\right), & (x \in \mathbb{R}, t > 0) \\ 0, & (x \in \mathbb{R}, t < 0) \end{cases} \quad (1.6)$$

and for any initial value problem

$$\begin{cases} \frac{\partial T}{\partial t} = \alpha^2 \frac{\partial^2 T}{\partial x^2}, & t > 0, \quad 0 < x < L, \\ T(x, 0) = g(x), & 0 < x < L, \end{cases}$$

its solution can be given as a convolution of $F(x, t)$ and $g(x)$; thus for $(x \in \mathbb{R}, t > 0)$ we have

$$T(x, t) = \frac{1}{2\alpha\sqrt{\pi t}} \int_{\mathbb{R}} \exp\left(-\frac{|x-y|^2}{4\alpha^2 t}\right) g(y) dy$$

Suppose that the equation (1.4) is associated with initial value, boundary values, and let all thermal parameters, density ρ , specific heat capacity c_p , and thermal conductivity κ be known, the problem of computing the temperature distribution throughout the body material is well-posed problem and is known as the *direct problem*. However, the problem of finding the surface temperature, i.e surface condition for given measurements of temperature at one

or more boundary points is an *inverse problem* which is often found to be an ill-posed problem in practice, and the process of estimation of surface temperature of body material from its interior measurements is referred to us as *Inverse Heat Conduction Problem(IHCP)*, [5, 8, 9].

Furthermore, the author of [10] classified the heat conduction problem into the regions depicted in *Fig.1.2*, we can see that if the measurement points x' and x'' are different, the boundary conditions of each inverse problem can be obtained by solving the direct problem and use its solution as boundary conditions for each inverse problem for two sides and also when x' and x'' are the same then temperature and heat flux must be given, and two inverse problems exist.

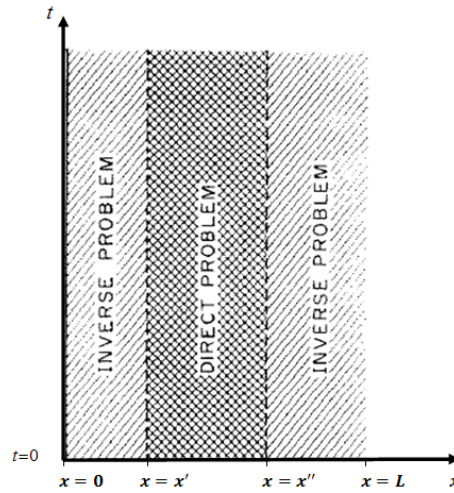


Fig. 1.2: Diagram of direct and inverse problem regions, adopted from [10]

The most types of inverse problems which have been raised in heat conduction were studied and summarized as: the problem of computing initial temperature from given temperature measurements, problem of computing the thermal parameters from given temperature measurements, and the problem of computing temperature of inaccessible part of the boundary from heat flux and temperature measurements on other parts of the boundary, [9].

The later problem is often occurred in practice, in the industries which produce and refine steels where the temperature and heat rates should be controlled at several stages during production to achieve good quality of the their products and also increase their economic level. However, in physical practice the surface may be impossible for attaching a sensor for taking measurements, or the accuracy of measuring surface temperature history may be seriously for some reason affected by that sensor; in that case solving an inverse heat conduction problem which consist of estimating the surface temperature from the temperature measurements made at an arbitrary location inside the metal should be used. The sensor can be a thermocouple if accessing the surface of the body material is possible, [2, 11, 12].

1.1.2 Methods of solving IHCP

The methods for solving heat conduction problem have been discussed and studied in literature. For instance, the classical methods for solving IHCP are based on transforming the problem into first-kind Volterra integral equations which is the type of problem that occur naturally in many applications and then combined with some regularization technique such as Tikhonov regularization, [13, 14]. And the disadvantage of the method is that the kernel of integration is not known explicitly when the material properties, thermal conductivity, κ and density, ρ are dependent on the temperature, [12].

In addition, Meyer and Daubechies wavelets and Fourier transform methods have been used to solve IHCP, where the partial differential equation was transformed into an initial value problem for an ordinary differential equation(ODE) by replacing the time derivative in the heat equation by wavelet-based approximations or a Fourier-based approximation, and then the resulting system of ODE was solved using standard numerical methods, such as Runge Kutta method, [15]. There exist also in literature other methods such as discrete mollification method that was proposed to solve the IHCP, see [16], the exact solution method which consisted of finding the solution as rapidly convergent series have been established in [17], and as well the finite differences, finite elements, and finite volume based methods for both linear and non linear problem were proposed, [4, 5, 18]. Thus, this thesis is based on the Crank-Nicolson implicit scheme finite difference and Tikhonov regularization.

1.1.3 Ill-posedness of IHCP

It has been argued that estimation of surface temperature of body material given its interior measurements is an inverse problem that has been studied by several authors for instance, [5, 10, 19] and it was found to be *ill-posed*, in the sense that small perturbations in the measurements lead to higher perturbations in resulting solutions. To understand the ill-posedness of inverse problem, let consider the operator equation problem

$$Kf = g \tag{1.7}$$

with K the bounded operator from subset X of classical spaces onto a subset Y , where X and Y are open subsets of $C^k(\Omega)$, $H_{k,p}(\Omega)$ or their finite co-dimensional subspaces, $f \in X$ and $g \in Y$ be unknown and known characteristics of heat model, respectively. The corresponding direct problem is given K and f then find g , and its corresponding inverse problem is given K and g , then find f .

Definition 1.1: *The problem is said to be well-posed if the following properties for given data hold:*

- (i) *Existence of solution, that is there exist $f \in X$ for any $g \in Y$*
- (ii) *Uniqueness of solution, that is such f in (i) is unique*

(iii) *Stability of solution*, that is $\|f - f^*\|_X \rightarrow 0$ as $\|g - g^*\|_Y \rightarrow 0$

Besides the problem (1.7) is said to be *well posed* when the operator K has bounded inverse operator K^{-1} from Y onto X . If one of those conditions defined in Definition 1.1 is not hold, the problem is said to be *ill-posed* and this is the more occurred case when solving the inverse heat conduction problem, [5, 9, 20, 21].

In [9, 20] the authors suggested that when the problem is ill-posed the property (i) can be neglected since one cannot suggest the conditions that will guarantee existence of solution even if the existence of solution is necessary, and also if the property (ii) is not holds this will leads to the problem of choosing the best solution among all solutions, final if the property (iii) is not holds, this will leads to a severe problem in numerical solution, since we are solving the problem with any small change in the data that will cause the higher change in the solution. Thus, the one way to handle this issue is to change the subspace X or to regularize the solution.

1.2 Background of the problem

1.2.1 Statement of the problem

We can write the problem (1.7) above as

$$K(f) = g, \quad f \in X \quad (1.8)$$

where $K : X \rightarrow Y$ is the mapping defined on X and taking values in Y . Let consider, X as the *solution space*, Y as the *space of exact data i.e right hand side*, and also let \hat{Y} be the *space of noisy measurements*, g^δ of g with noise level δ the standard deviation of Gaussian white noise says η . In this thesis we would like to approximate a solution of the ill-posed problem (1.8) with given right-hand side $g^\delta \in \hat{Y}$, i.e, $K(f) = g^\delta$ numerically. Here, *ill-posedness* is in the sense of Definition 1.1 that the solutions do not depend continuously on the data and in our practice, existence of solutions will be assumed and uniqueness is not of interest since in practice and theory we obtain multiple solutions and we choose the best one. Since, the exact data $g \in Y$ are not available, but its noisy version $g^\delta \in \hat{Y}$ is available and small discretization or rounding errors this can yield to arbitrarily large difference between the numerical solution and the exact solution.

Therefore, solving an *ill-posed problem* numerically require much effort to deal with the that ill-posedness. Due to the fact that g^δ is very sensitive to perturbations, then this issue can be coped by solving the following minimization problem

$$\min_{f \in X} \Phi(K(f), g^\delta) \quad (1.9)$$

instead of problem (1.8), where $\Phi : Y \times \hat{Y} \rightarrow [0, \infty)$ is some *fitting functional* for instance $\Phi(K(f), g^\delta) := \|K(f) - g^\delta\|_2^2$, which is the minimal least-squares (LS) problem, [22]. Furthermore, if the problem (1.8) is ill-posed then its corresponding minimization problem (1.9)

will be also ill posed; so to cope with that issue we can add some *penalty function* $J(f)$ to $\Phi(K(f), g^\delta)$ and obtain the new minimization problem

$$\min_{f \in X} \left\{ \Phi(K(f), g^\delta) + \lambda^2 J(f) \right\} \quad (1.10)$$

where $J(f) : X \rightarrow \mathbb{R}$ and λ is some positive *regularization parameter*. This problem (1.10) is known as *Tikhonov regularized problem*, which is discussed in more details in Section 2.4.1 and the Tikhonov problem is given in the equation (2.46). Besides of this description of the problem the following Section (1.2.2) of application explain in details the main problem we have in hand in the thesis.

1.2.2 Application

In applications it is often of importance to find the temperature on the surface of an object in situations where the surface itself is inaccessible for direct measurement. This is the case for instance when studying heat treatment of steel. The process is strongly influenced by the time dependent temperature and heat-flux close to the surface. In such applications one can place a measurement point inside the body material, close to the surface, and compute the surface temperature by solving a heat conduction problem in the region between the measurement point and the surface, [12]. The *Fig.2.3* illustrate the situation.

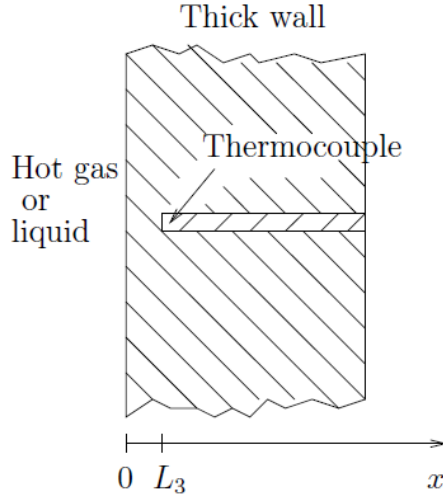


Fig. 1.3: Determination of surface temperature from interior measurements

A simple mathematical model that describe the situation is

$$\begin{cases} \rho c_p \frac{\partial T(x,t)}{\partial t} = \frac{\partial}{\partial x} \left(\kappa(x) \frac{\partial T(x,t)}{\partial x} \right), & t \geq 0, 0 \leq x \leq L_3 \\ T(x, 0) = T_0 = \text{constant}, & 0 \leq x \leq L_3 \\ T(0, t) = f(t), & t \geq 0 \\ T(L_3, t) = g_3(t), & t \geq 0 \end{cases} \quad (1.11)$$

where $T(x, t)$ is the temperature distribution inside the body material which is governed by heat conduction equation (1.4), $T(0, t) = f(t)$ is the surface temperature for $t \geq 0$, and $T(L_3, t) = g_3(t)$ is the temperature recorded by the measurement device for $t \geq 0$ and $x = L_3$. Initially the temperature can be taken to be constant. In this thesis we consider the case where the steel material is heated to a constant temperature before the heat treatment starts, then we have $T(x, 0) = g_3(0) = f(0)$, for $0 \leq x \leq L_3$.

As we will show later that if we take the model (1.11) with its initial and boundary conditions as described above then the problem of finding $T(x, t)$ is *well-posed*. Then it can be solved using standard numerical methods.

In fact, in our application we want to determine the surface temperature, i.e. $f(t)$ is unknown. In order to accomplish this we take additional measurement, i.e, we recorded the temperature at one additional location, see *Fig.2.2*, $T(L_2, t) = g_2(t)$ for $t \geq 0$, and $0 < L_2 < L_3$.

By solving the well-posed problem in the interval $0 \leq x \leq L_3$ using $f(t)$ and $g_3(t)$ as boundary values we can compute the temperature at the location $x = L_2$.

This can be formally used to define an operator \widetilde{K} by $\widetilde{K}(g_3)f(t) = T(x = L_2, t) = g_2(t)$. Therefore, for given measurement $g_2^\delta(t)$ we could consider the problem of finding $f(t)$ as an operator equation, $\widetilde{K}(g_3)f(t) = g_2^\delta(t)$, and solve for the unknown surface temperature $f(t)$. This approach works well with some complications that need to be dealt with. We show later that:

- The problem of finding $f(t)$ from the measurements g_2^δ and g_3^δ is *ill-posed* and regularization is needed.
- The operator \widetilde{K} is non-linear;

and however most efficient regularization methods are designed for solving linear operator equations, for instance in [23, 24, 25]. Therefore, in this project the operator equation, $\widetilde{K}(g_3)f(t) = g_2^\delta(t)$, was rewritten as a linear operator equation, $Kf(t) = g_2^\delta(t)$, we investigated the *ill-posedness* of the problem, and also we solved it using an efficient regularization method. Finally, the developed method was applied to a real industrial problem with measured data taken during an industrial steel quenching process in [12].

To improve the accuracy of the solution, we included more measurements as follows: The third measurement point, located at $x = L_1$ was included, for instance see *Fig.3.3(a)*, and redefine the linear operator equation $Kf(t) = T(L_2, t) = g_2^\delta(t)$ as $Kf(t) = (T(L_1, t), T(L_2, t)) = (g_1^\delta, g_2^\delta)$ and apply the same regularization technique. Impact of using the additional data on the estimate of the surface temperature and the stability of the inverse problem is investigated. We find out that it improves the estimate of the surface temperature and stability of the inverse problem.

1.3 Objective

First standard theory for the inverse heat conduction problem was studied and summarized as an introductory part of the thesis. The specific objectives are:

1. To write a finite difference solver that can solve the direct well-posed problem as described above. Also write a code for evaluating the linear operator K .
2. To apply Thikhonov regularization to the linear operator equation to find the numerical approximation of the surface temperature $f(t)$ and investigate the properties of the problem, e.g. stability and accuracy, numerically
3. To reformulate the operator equation to include more data and also update the finite difference solvers for this situation.
4. To apply the developed software to an industrial situation and find the surface temperature during a quenching process using measured data.

1.4 Related works

The problem of estimating surface temperature or surface heat flux based on the measurements of temperature at some interior points have aroused the curiosities of several researchers, and was found to be an ill posed and was known to us as an inverse heat conduction problem. Such case can happen in different area of studies, for instance in aerodynamic studies, quenching studies, and in laboratories which use indirect calorimetry devices; thus this chapter review the existing literature for addressing such mentioned problem.

In the literature there are exact solutions and numerical solutions of inverse heat conduction problem (IHCP). One of 1900s written papers on IHCP was about solving numerically an inverse problem of heat conduction for simple shapes as in application in quenching process with special reference to the sphere of r , r_1 and R distance from center, particular values of r and outer radius respectively and was published in 1960 by Soltz. The problem author had in hand was the following: the temperature of the body was initially uniform, and the temperature $\theta(r_1, \tau)$ at some interior point r_1 as a function of time was known and tried to find the surface heat flux and surface temperature, $Q(t) = -\kappa(R, t)/\partial r$ and $T(R, t)$, from the following problem (1.12)

$$\begin{cases} \alpha \nabla^2 T(r, t) - \frac{\partial T}{\partial r} = 0; & 0 \leq r < R \\ \frac{\partial}{\partial r} T(0, t) = 0 \\ T(r, 0) = T_i; & \text{constant} \\ T(r_1, t) = f(t); & 0 \leq r_1 < R \end{cases} \quad (1.12)$$

and then to solve the problem the author formulated the problem as it was direct one, obtain its integral equation for unknown surface condition and thus the numerical solution was obtained by inverting that integral equation, [26]. Thereafter, in 1964 other work was published on numerical integration method to solve an inverse problem in transient heat conduction problem which gave a solution method that is more general and which may be computationally simpler, and the theory was able to accommodate a nonuniform initial temperature distribution within the solid. In addition analytical treatment was extended to the sphere, the plane slab, and the long cylinder, [27]. Also the exact solution of the inverse problem in heat conduction theory and application was established by Buggraf in the form of rapidly convergent series of all-order derivatives of both temperature $T(x, t)$ and heat flux $Q(t)$, [17].

In 1996, the numerical solution of generalized IHCP by using discrete mollification method was obtained in [16] and for more details on mollification method to solve the ill-posed problems see, [28].

Furthermore, in 1999 the author of [8] used the spectral method to solve the inverse heat conduction problem (1.13) known as sideways heat equation and this problem was found to be an ill-posed problem, thus the problem was stabilized by introducing the cutting off high frequencies in the Fourier space domain.

$$\begin{cases} \kappa T_{xx} = T_t; & 0 < x < 1, t \geq 0 \\ T(1, t) = g(t); & t \geq 0 \\ T_x(1, t) = h(t); & t \geq 0 \\ T(x, 0) = 0; & 0 \leq x \leq 1 \end{cases} \quad (1.13)$$

The solution of (1.13) in the Fourier domain was easily found to be

$$\hat{T}(x, \xi) = \frac{1}{2}(e^{\sqrt{i\xi/\kappa(1-x)}}(\hat{g} - \hat{h}/\sqrt{i\xi/\kappa}) + \frac{1}{2}(e^{-\sqrt{i\xi/\kappa(1-x)}}(\hat{g} + \hat{h}/\sqrt{i\xi/\kappa}))$$

where h is the heat-flux measurements, $\hat{T}(x, \xi)$ is the Fourier transform of $T(x, t)$, and ξ is the parametrization parameter. The cut-off frequency ξ_c was introduced and all high frequencies were drawn away in the solution, and thus the regularized solution $T(x, t)$ can be obtained by taking Fourier inverse transform of equation (1.14),

$$\hat{T}_c(x, \xi) = \chi_c(\xi)\hat{T}(x, \xi) \quad (1.14)$$

with χ_c the characteristic function of $[-\xi_c, \xi_c]$. Moreover, the problem (1.13) was discretized separately in time and in space domain. By using the method of lines the initial value problem of an ordinary differential equation was obtained and solved numerically by implementing fourth-order Runge Kutta method, where the time derivative was approximated by using discrete Fourier transform.

2. ESTIMATION OF SURFACE TEMPERATURE

We have argued that the problem of determining the surface temperature $f(t)$ from some arbitrary measurement points taken inside of the body material as described in Section 1.2.2 above is an *inverse problem*. Let recall here what is an inverse problem. Following [9] an inverse problem is concerned with knowing the present state of the system from future observations, that is the calculation of the evolution of the system backwards in time. Also an inverse problem can denotes the task of computing an unknown physical quantity of the system form indirect measurements. Simply the inverse problem consisting of determining the *causes* knowing the *effects* as shown in *Fig.2.1*.

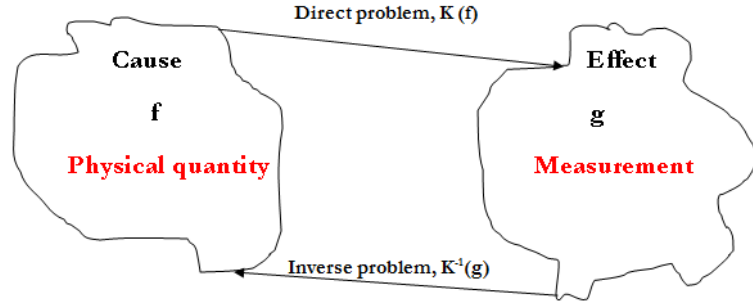


Fig. 2.1: Direct and Inverse problem diagram

In this thesis, the inverse problem we have is to find the surface temperature $T(0, t) = f(t)$ for given measurements $T(L_3 = 1, t) = g_3(t)$ and additional extra boundary condition $T(L_2, t) = g_2(t)$ on the mathematical model (1.11) where the bounded time interval $0 \leq t \leq 1$ is used since in practice we can only collect measurements during a finite time interval. And $T(x, t)$ satisfies the following resulting problem written in its simplified form. Now

$$\left\{ \begin{array}{l} (a(x)T_x)_x = T_t, \quad 0 \leq t \leq 1, \quad 0 \leq x \leq 1 \\ T(x, 0) = T_0 = \text{constant}, \quad 0 \leq x \leq 1 \\ T(0, t) = f(t), \quad 0 \leq t \leq 1 \\ T(1, t) = g_3(t), \quad 0 \leq t \leq 1 \\ T(L_2, t) = g_2(t), \quad 0 < L_2 < 1, \quad 0 \leq t \leq 1 \end{array} \right. \quad (2.1)$$

We can note that the problem of finding the solution $T(x, t)$ with given boundary conditions is *well posed problem* in the region $L_2 < x < 1$ but an *ill-posed problem* in the region $0 < x < 1$.

Furthermore, $a(x)$ was used instead of using ρ , c_p and $\kappa(x)$ as in general problem (1.11) since this is a theoretical study and $a(x)$ changes as x changes thus the results could arrive to the same results as for using thermal properties of the material. Based on Section 1.1.3, the computation of $T(0, t) = f(t)$ in this case is an *ill-posed problem* and our space and time grid domains are $0 \leq x \leq 1$ and $0 \leq t \leq 1$, respectively.

2.1 A Linear operator equation and its properties

Since our purpose is to determine the unknown surface temperature $T(0, t) = f(t)$ from the problem (2.1) with given measurement temperature $T(L_3, t) = g_3(t)$, to do so we record the temperature at one additional location $x = L_2$, $T(L_2, t) = g_2(t)$ as shown in *Fig.2.2* below. And then given a measurement $g_2(t)$ we could consider the problem of finding $f(t)$ as an operator equation such that $\tilde{K}(g_3)f(t) = g_2(t)$, and solve for $f(t)$ where the operator $\tilde{K}(g_3)$ is defined in Definition 2.2 below; but let us first define the function space which is considered throughout this thesis where the functions f and g_2 belong.

Definition 2.1: (**Function space** $C^0([a, b])$) We denote $C^k([a, b])$, $0 \leq k \leq \infty$ the space of real valued k -times continuously differentiable functions on the closed interval $[a, b]$ of \mathbb{R} . Thus, the most common $C^k([a, b])$ space is $C^0([a, b])$ the space of continuous functions defined as $C^0([a, b]) = \{f : [a, b] \rightarrow \mathbb{R} : f(t) \text{ continuous on } [a, b]\}$. This can be found in [29, 30] or any standard book of functional analysis.

Throughout the remaining part of the thesis we consider the closed interval $[a, b]$ to be $[0, 1]$, and for the real-valued functions f and $g_2 \in C^0([0, 1])$, we define the possible metrics and norms that can be defined on $C^0([0, 1])$.

(a) We define a uniform metric on $C^0([0, 1])$ by

$$\rho_\infty(f, g_2) = \max_{t \in [0, 1]} |f(t) - g_2(t)|, \quad (2.2)$$

, and the corresponding norm of $f(t)$ is given by

$$\|f\|_\infty = \max_{t \in [0, 1]} |f(t)| \quad (2.3)$$

(b) We define also, for a fixed real number $p \geq 1$, the metric on $C^0([0, 1])$

$$\rho_p(f, g_2) = \left(\int_0^1 |f(t) - g_2(t)|^p dt \right)^{\frac{1}{p}},$$

and the correspond norm of $f(t)$ is given by

$$\|f\|_p = \left(\int_0^1 |f(t)|^p dt \right)^{\frac{1}{p}}$$

Lemma 2.1: *The function space $C^0[0, 1]$ equipped with maximum norm, $\|\cdot\|_\infty$ is Banach space.*

Proof: Let $\{f_m(t)\} \subset C^0([0, 1])$ and $\{f_m(t)\}$ be a Cauchy sequence in $C^0([0, 1])$, then

$$\|f_m - f_n\| = \max_{t \in [0, 1]} |f_m(t) - f_n(t)| < \epsilon, \text{ for } (m, n > N(\epsilon)) \quad (2.4)$$

Hence, for any fixed $t = t_0 \in [0, 1]$, we get $\|f_m(t_0) - f_n(t_0)\| < \epsilon$, for $(m, n > N(\epsilon))$, so $\{f_m(t_0)\}$ is a Cauchy sequence in \mathbb{R} . And \mathbb{R} being complete, see [30], we can assign to each $t \in [0, 1]$ a unique $f(t) \in \mathbb{R}$ which define a pointwise function f on $[0, 1]$. For $t \in [0, 1]$ and let $n \rightarrow \infty$ in equation (2.4) we have

$$\|f_m - f\| < \epsilon, \text{ for } (m > N(\epsilon)) \quad (2.5)$$

This shows that the sequence $\{f_m\}$ of continuous functions converges uniformly to the function f on $[0, 1]$, and hence the limit function f is a continuous function on $[0, 1]$. Also from equation (2.5) we have

$$\max_{t \in [0, 1]} |f_m(t) - f(t)| < \epsilon, \text{ for } (m > N(\epsilon))$$

which implies that $\|f_m - f\| < \epsilon$, for $(m > N(\epsilon))$, and then $f_m \rightarrow f \in C^0([0, 1])$. Thus, $C^0([0, 1])$ is Banach space, [31].

Definition 2.2: *We define the operator $\widetilde{K}(g_3) : C^0([0, 1]) \rightarrow C^0([0, 1])$ such that $(\widetilde{K}(g_3)f)(t) = T(x = L_2, t) = g_2(t)$, where $T(x, t)$ is the solution of the problem (2.1), f and g_2 are continuous functions over $[0, 1]$ and $0 < L_2 < 1$ as shown in Fig.2.2*

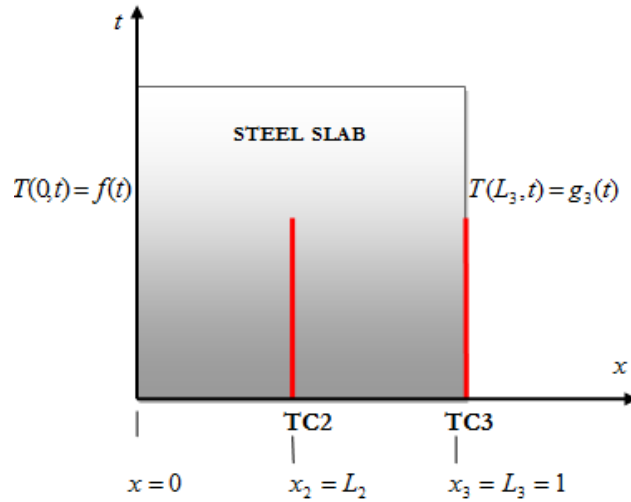


Fig. 2.2: *The positions of the thermocouples TC2, and TC3 inside the material that can be used to measure the temperature histories in practice*

In order to study the properties of the operator $\widetilde{K}(g_3)$ we split the problem (2.1) into the following two sub-problems:

$$\begin{cases} (a(x)T_x^a)_x = T_t^a, & 0 \leq t \leq 1, 0 \leq x \leq 1 \\ T^a(0, t) = f(t), & 0 \leq t \leq 1 \\ T^a(x, 0) = 0, & 0 \leq x \leq 1 \\ T^a(1, t) = 0, & 0 \leq t \leq 1 \\ T^a(L_2, t) = \widetilde{g}_2(t), & 0 \leq t \leq 1 \end{cases} \quad (2.6)$$

and

$$\begin{cases} (a(x)T_x^b)_x = T_t^b, & 0 \leq t \leq 1, 0 \leq x \leq 1 \\ T^b(0, t) = 0, & 0 \leq t \leq 1 \\ T^b(x, 0) = T_0 = \text{constant}, & 0 \leq x \leq 1 \\ T^b(1, t) = g_3(t), & 0 \leq t \leq 1 \\ T^b(L_2, t) = g_2(t) - \widetilde{g}_2(t), & 0 \leq t \leq 1 \end{cases} \quad (2.7)$$

We first find $T^b(x, t)$ that satisfies (2.7), and then since the heat equation is linear function we can note that $T^a(x, t)$, solution to the problem (2.6) can be written as $T^a(x, t) = T(x, t) - T^b(x, t)$ where $T(x, t)$ satisfies the problem (2.1) with $\widetilde{g}_2(t) = T(L_2, t) - T^b(L_2, t) = g_2(t) - T^b(L_2, t)$. Moreover, the problem (2.6) is known to be *well-posed* so it can be reformulated as an operator equation such that $(Kf)(t) = T^a(x = L_2, t) = \widetilde{g}_2(t)$ where K is an operator defined as follows:

Definition 2.3: We define the operator $K : C^0([0, 1]) \rightarrow C^0([0, 1])$ that maps $f(t)$ to $\widetilde{g}_2(t) = T^a(x = L_2, t)$, that is $(Kf)(t) = \widetilde{g}_2(t)$ where $T^a(x, t)$ is the solution of the problem (2.6), f and \widetilde{g}_2 are continuous functions over $[0, 1]$, and $0 < L_2 < 1$.

Lemma 2.2: (Linearity) The operator K defined in Definition 2.3 is linear; that is the following properties hold:

(i) *Additive:* $(K(s + h))(t) = (Ks)(t) + (Kh)(t)$, for the surface temperature s and $h \in C^0([0, 1])$

(ii) *Homogeneous:* $(K(\alpha f))(t) = \alpha(Kf)(t)$, for positive real number α and $f \in C^0([0, 1])$

Proof: (i) Let $T_{sh}^a(x, t) = T_s^a(x, t) + T_h^a(x, t)$ be the solution of problem (2.6) where the boundary condition $f(t) = T^a(0, t)$ is replaced by $r(t) = s(t) + h(t)$ and $T_s^a(x, t)$ and $T_h^a(x, t)$ be the solutions of problem (2.6) where $f(t)$ is replaced by $s(t)$ and $h(t)$, respectively. It is clear that by Definition 2.3 that

$$\begin{aligned} (Kr)(t) &= (K(s + h))(t) \\ &= \widetilde{l}_2(t) + \widetilde{j}_2(t) \\ &= (Ks)(t) + (Kh)(t) \end{aligned}$$

where $\tilde{l}_2(t)$ and $\tilde{j}_2(t)$ are the functions such that the operator K maps $s(t)$ and $h(t)$ to $\tilde{l}_2(t)$ and $\tilde{j}_2(t)$, respectively. The result shows that for $x = 1$ we have $T_s^a(1, t) + T_h^a(1, t) = 0 + 0 = 0$ hence the boundary condition $T^a(1, t) = 0$ is also satisfied, therefore the operator K is additive.

To prove (ii) let $T^a(x, t)$ be amplified by positive real number α , then the problem (2.6) become

$$\left\{ \begin{array}{l} (a(x)T_x^a)_x = T_t^a, \quad 0 \leq t \leq 1, \quad 0 \leq x \leq 1 \\ \alpha T^a(0, t) = f(t), \quad 0 \leq t \leq 1 \\ T^a(x, 0) = 0, \quad 0 \leq x \leq 1 \\ T^a(1, t) = 0, \quad 0 \leq t \leq 1 \\ \alpha T^a(L_2, t) = \tilde{g}_2(t), \quad 0 \leq t \leq 1 \end{array} \right. \quad (2.8)$$

We can note that solving problem (2.8) is equivalent to solve problem (2.6) where $T^a(x, t)$ is replaced by $\alpha T^a(x, t)$. It follows that

$$\begin{aligned} (K(\alpha f))(t) &= \alpha T^a(x = L_2, t) \\ &= \alpha \tilde{g}_2(t) \\ &= \alpha (Kf)(t) \end{aligned}$$

The last equality hold since $\tilde{g}_2(t) = (Kf)(t)$ which shows that the operator K is homogeneous.

Remark 2.1: *The operator $\tilde{K}(g_3)$ defined in Definition 2.2 is non linear*

Proof: From Definition 2.2 and 2.3 it follows that

$$\begin{aligned} (\tilde{K}(g_3)f)(t) &= T(x = L_2, t) \\ &= T^a(x = L_2, t) + T^b(x = L_2, t) \\ &= (Kf)(t) + T^b(x = L_2, t) \end{aligned}$$

Where K is the linear operator defined in Definition 2.3 and $T^b(x, t)$ is the solution of sub-problem (2.7) which depends on initial temperature T_0 and the temperature at the boundary $x = L_3, g_3(t)$. In fact, we see that $\tilde{K}(g_3)$ is an affine operator, by assuming that $T^b(x = L_2, t)$ is known.

Proposition 2.1: *The problem of finding the solution $T(x, t)$ that satisfies the problem (2.1) for given initial and boundary conditions is the direct problem which is well-posed problem. That is there exist at least one such $T(x, t)$, which should be at most one, and finally continuously depends on the data of the problem.*

Proof: First we prove the uniqueness of $T(x, t)$. Let us assume that there exist two different solutions, $T_1(x, t)$ and $T_2(x, t)$ of the problem (2.1) and also define $u(x, t) = T_1(x, t) - T_2(x, t)$ to be their difference. And let us define the energy function associated with $u(x, t)$ as follows:

$$E(t) := \int_0^1 u^2(x, t) dx \quad (2.9)$$

According to the *superposition principle*, $u(x, t)$ must also be the solution to the problem (2.1). Then we have:

$$\begin{cases} (a(x)u_x)_x = u_t, & 0 \leq t \leq 1, 0 \leq x \leq 1 \\ u(x, 0) = 0, & 0 \leq x \leq 1 \\ u(0, t) = 0, & 0 \leq t \leq 1 \\ u(1, t) = 0, & 0 \leq t \leq 1 \\ u(L, t) = 0, & 0 \leq t \leq 1 \end{cases} \quad (2.10)$$

We need to show that $T_1(x, t)$ and $T_2(x, t)$ are identical. To do so let multiply the above partial differential equation given in (2.10) by $u(x, t)$ and integrate both sides with respect to x in the domain $0 \leq x \leq 1$, this can be simply written as:

$$\int_0^1 u_t u dx = \int_0^1 (a(x)u_x)_x u dx \quad (2.11)$$

By integrating by part the right hand side of the equation (2.11) we have

$$\int_0^1 u_t u dx = [a(x)u_x u]_0^1 - \int_0^1 a(x)u_x^2 dx \quad (2.12)$$

By using the boundary conditions, $u(0, t) = u(1, t) = 0$, given in (2.10) and simplifying the left hand side of (2.12) we get

$$\int_0^1 \left(\frac{1}{2} u^2 \right)_t dx = - \int_0^1 a(x)u_x^2 dx \quad (2.13)$$

Let assume that $u(x, t)$ and $u_t(x, t)$ are continuous functions, then the time derivative in equation (2.13) can be pulled out and thus we have

$$\frac{d}{dt} \int_0^1 \left(\frac{1}{2} u^2 \right) dx = - \int_0^1 a(x)u_x^2 dx \leq 0 \quad (2.14)$$

Since, the right hand side of equation (2.14) is less than or equal to zero, hence $\int u^2(x, t) dx$ is decreasing function of time. Then

$$\int_0^1 u^2(x, t) dx \leq \int_0^1 u^2(x, 0) dx \quad (2.15)$$

for $t \geq 0$. By using the initial condition, $u(x, 0) = 0$, we have $\int u^2(x, t) dx = 0$. Therefore $u(x, t) \equiv 0$ and $T_1(x, t) = T_2(x, t)$ for $t \geq 0$. Therefore, if $T(x, t)$ exist should be unique.

Secondary, we need to prove the stability of the problem, that is the initial and boundary conditions are well formulated. Here we use also the energy method by assuming that $T(0, t) = T(1, t) = 0$ and the initial temperature to be a function of x , i.e $T(x, 0) = \zeta(x)$. Let $T_1(x, 0) = \zeta_1(x)$ and $T_2(x, 0) = \zeta_2(x)$, then $u(x, t) = T_1(x, t) - T_2(x, t)$ is the solution with initial value temperature $[\zeta_1(x, 0) - \zeta_2(x, 0)]$. Then from equation (2.15) we get the stability in square integral sense, that is

$$\int_0^1 (T_1(x, t) - T_2(x, t))^2 dx \leq \int_0^1 (T_1(x, 0) - T_2(x, 0))^2 dx \quad (2.16)$$

Then from equation (2.16) we can note that the variation in the solutions at any later time is less than the variation in the initial data for two solutions, since the quantities on left side and right side of (2.16) measure the nearness of the solutions at any later time and the nearness of the initial data for two solutions, respectively. Therefore, if we start nearby $t = 0$, we stay nearby. Hence, any small perturbation in the initial data will result to the small perturbation in the solution.

Remark 2.2: *Here in the thesis we discussed the stability of the problem (2.1) by using initial condition $T(x, 0)$. However, the effects of disturbance in the boundary conditions, i.e $x = 0$ and $x = 1$ should be also addressed, but we refer to [6] where the maximum principle have been used to show that disturbances.*

Proposition 2.2: (Shift invariance) *The operator K defined in Definition 2.3 is time shift invariant i.e $Kf(t - t_0) = \widetilde{g}_2(t - t_0)$ for $t_0 > 0$.*

Proof: Let for t_0 , $\widehat{f}(t) = f(t - t_0)$ be the boundary condition of the problem (2.6) at $x = 0$ for time $(t - t_0)$ and due to the initial condition we have $f(0) = \widetilde{g}_2(0) = 0$ and also $\widetilde{g}_2(0) = \widehat{f}(0)$ is valid solution. By Definition 2.3, it follows that

$$\begin{aligned} (K\widehat{f})(t) &= (Kf)(t - t_0) \\ &= \widetilde{g}_2(t - t_0) \end{aligned}$$

then for $\widehat{f}(t)$, $(K\widehat{f})(t) = \widehat{g}_2(t)$ where $\widehat{g}_2(t) = \widetilde{g}_2(t - t_0)$.

2.2 Discretization using finite differences

In this section we seek to approximate the partial differential equation given in (2.6) with another expression which prescribe values at only a finite number of discrete points of some given space and time domains. Thus, in this thesis the finite difference method which consists on replacing the derivatives in differential equations with finite difference approximations was used. This method is based on Taylor's series expansions. This gave a large finite algebraic

system of equation to be solved instead of partial differential equation, and the computer is needed to find its numerical solution with some initial condition and boundary conditions on the boundaries of those domains, [18, 32, 33, 34].

Assume that the function $T(x, t)$ is sufficiently smooth function in x and in t and define the equidistant grid space and time domains $\Omega = \{x|x = x_i = i\Delta x, i = 0, 1, \dots, n; \text{ for } n\Delta x = 1\}$ and $\Omega' = \{t|t = t_j = j\Delta t, j = 0, 1, \dots, N; \text{ for } N\Delta t = 1\}$ with space and time step size Δx and Δt on the interval $[0, 1]$, respectively.

Let T_i^j denotes $T(x, t)$ at point (x_i, t_j) , thus T_{i-1}^j and T_{i+1}^j can be calculated in terms of Taylor series expansion of $T(x, t)$ around the arbitrary point (i, j) i.e (x_i, t_j) just to simplify the notation. Hence,

$$T_{i\pm 1}^j = T_i^j \pm \Delta x (T_x)_i^j + \frac{(\Delta x)^2}{2} (T_{xx})_i^j \pm \frac{(\Delta x)^3}{3!} (T_{xxx})_i^j + O((\Delta x)^4) \quad (2.17)$$

From the equation (2.17) we approximate $(T_x)_i^j$ by using left difference derivative noted as $\tilde{T}_{\bar{x}}$ here

$$\tilde{T}_{\bar{x}} \equiv \frac{T_i^j - T_{i-1}^j}{\Delta x} = (T_x)_i^j - \frac{\Delta x}{2} (T_{xx})_i^j + O((\Delta x)^2) \quad (2.18)$$

The same from the equation (2.17) we approximate $(T_x)_i^j$ by using right difference derivative noted as \tilde{T}_x here

$$\tilde{T}_x \equiv \frac{T_{i+1}^j - T_i^j}{\Delta x} = (T_x)_i^j + \frac{\Delta x}{2} (T_{xx})_i^j + O((\Delta x)^2) \quad (2.19)$$

In addition $(T_x)_i^j$ can be obtained by using central difference formula and then it can be written as

$$(T_x)_i^j = \frac{T_{i+1}^j - T_{i-1}^j}{2\Delta x} + O((\Delta x)^2) \quad (2.20)$$

which is second order *central difference* equation. And also $(T_{xx})_i^j$ can be approximated by summing the left finite derivative and right finite derivative of $T(x, t)$ from equation (2.17) and solve for $(T_{xx})_i^j$ this yield a second order accurate *central finite difference* equation

$$(T_{xx})_i^j = \frac{T_{i+1}^j - 2T_i^j + T_{i-1}^j}{(\Delta x)^2} + O((\Delta x)^2) \quad (2.21)$$

Moreover, $(T_t)_i^j$ can be approximated using for instance forward difference equation as

$$(T_t)_i^j = \frac{T_i^{j+1} - T_i^j}{\Delta t} + O(\Delta t) \quad (2.22)$$

Now, the partial differential equation given in the problem (2.6) rewritten below as

$$T_t = (a(x)T_x)_x, \quad a(x) > 0 \quad (2.23)$$

can be reduced to

$$T_t = a(x)_x T_x + a(x) T_{xx}, \quad a(x) > 0 \quad (2.24)$$

The discrete form of equation (2.23) is obtained follows the same approach used in [18] by defining the one-dimensional operator

$$AT = (a(x)T_x)_x \quad (2.25)$$

and use the difference expression

$$(a(x)T_x)_x = \frac{a_{i+1}}{\Delta x} \tilde{T}_x - \frac{a_i}{\Delta x} \tilde{T}_x \quad (2.26)$$

with \tilde{T}_x and \tilde{T}_x defined in equation (2.18) and (2.19), respectively. Therefore by consider, equations (2.18) and (2.19) we get the following

$$(a(x)T_x)_x = \frac{a_{i+1} - a_i}{\Delta x} (T_x)_i + \frac{a_{i+1} + a_i}{2} (T_{xx})_i + O((\Delta x)^2) \quad (2.27)$$

Thus, the coefficient a_i can be obtained by comparing the equations (2.24) and (2.27) which yield to

$$\frac{a_{i+1} - a_i}{\Delta x} = a(x)_x + O((\Delta x)^2) \quad (2.28)$$

$$\frac{a_{i+1} + a_i}{2} = a(x) + O((\Delta x)^2) \quad (2.29)$$

Hence, the dicritization of equation (2.23) is obtained by inserting equation (2.22), (2.21), (2.28), and (2.29) into equation (2.24) and obtain the following:

$$\left(\frac{T_i^{j+1} - T_i^j}{\Delta t} \right) = \frac{a_{i+1} - a_i}{2(\Delta x)^2} (T_{i+1}^j - T_{i-1}^j) + \frac{a_{i+1} + a_i}{2(\Delta x)^2} (T_{i+1}^j - 2T_i^j + T_{i-1}^j) \quad (2.30)$$

After some rearrangement of equation (2.30) we obtain

$$T_i^{j+1} = ra_i T_{i-1}^j + [1 - r(a_{i+1} + a_i)] T_i^j + ra_{i+1} T_{i+1}^j \quad (2.31)$$

where $r = \Delta t/(\Delta x)^2$, for $i = 1, 2, \dots, n$ and $j = 0, 1, \dots, N$ and this gives an **explicit method** for solving the given partial differential equation.

Despite the fact that the explicit method given in equation (2.31) is simple to be implemented it has one serious disadvantage, that is the time step Δt should be necessarily very small because the method is conditional stable since the computationally process is valid only for $0 < \Delta t/(\Delta x)^2 \leq \frac{1}{2}$, thus Δx should be kept small as much as possible so that the method is valid. Therefore, Crank and Nicolson suggested in [35] a satisfactory method of numerical evaluation of solutions of partial differential equations of the heat conduction type and their method is unconditional stable for any $r > 0$, [32, 34].

Therefore, the scheme of the Crank-Nicolson to solve the partial differential equation is to consider partial differential equation as being satisfied at the point $(i\Delta x, (j + \frac{1}{2})\Delta t)$, in other words the partial derivatives are replaced by the mean of its finite difference approximations at j^{th} and $(j + 1)^{th}$ time levels, [32, 34, 35]. Thus, T_{i-1}^j , T_i^j , and T_{i+1}^j on right hand side of equation (2.31) are approximated by their average properties between time levels j^{th} and

$(j+1)^{th}$ and the coefficient a_i by their average between the space levels i^{th} and $(i+1)^{th}$ and perform some rearrangement, that yield the **Crank-Nicolson implicit scheme**:

$$-r\beta T_{i-1}^{j+1} + (2+r\nu)T_i^{j+1} - r\mu T_{i+1}^{j+1} = r\beta T_{i-1}^j + (2-r\nu)T_i^j + r\mu T_{i+1}^j \quad (2.32)$$

where $\beta = (a_{i+1} + a_i)$, $\nu = (a_{i+2} + 2a_{i+1} + a_i)$, and $\mu = (a_{i+2} + a_{i+1})$. When equation (2.32) is evaluated sequentially at each grid, then we get the following linear system of algebraic, with unknowns T_i^{j+1} for $i = 1, 2, \dots, (n-1)$ and $j = 0, 1, \dots, (N-1)$.

$$\begin{bmatrix} (2+r\nu) & -r\mu & & & \\ -r\beta & (2+r\nu) & -r\mu & & \\ & -r\beta & (2+r\nu) & -r\mu & \\ & & \ddots & \ddots & \ddots \\ & & & -r\beta & (2+r\nu) \end{bmatrix} \begin{bmatrix} T_1^{j+1} \\ T_2^{j+1} \\ \vdots \\ T_{n-2}^{j+1} \\ T_{n-1}^{j+1} \end{bmatrix} = \begin{bmatrix} (2-r\nu) & r\mu & & & \\ r\beta & (2-r\nu) & r\mu & & \\ & r\beta & (2-r\nu) & r\mu & \\ & & \ddots & \ddots & \ddots \\ & & & -r\beta & (2-r\nu) \end{bmatrix} \begin{bmatrix} T_1^j \\ T_2^j \\ \vdots \\ T_{n-2}^j \\ T_{n-1}^j \end{bmatrix} + \begin{bmatrix} 2T_0^j \\ 0 \\ \vdots \\ 0 \\ 2T_n^j \end{bmatrix} \quad (2.33)$$

Here T_0^j and T_n^j for all $j = 0, 1, \dots, N$ are known values from the boundary conditions and T_i^0 are known values for all $i = 0, 1, \dots, n$ from initial condition. The equation (2.33) can be written as $AT_i^{j+1} = BT_i^j$ where A and B are the matrices on the right hand side and left hand side of equation (2.33), respectively. We can note that the computation of T_i^{j+1} from the equation (2.33) the computer is needed, hence the author developed a MATLAB solver¹, that implement the Crank-Nicolson to compute the temperature distribution $T(x_i, t_j)$ in the material, that is temperature at each grid point (i, j) for given boundary conditions and initial condition.

2.3 Linear discrete problem

Let the problem (2.6) rewritten as

$$\begin{cases} (a(x)T_x)_x = T_t, & 0 \leq t \leq 1, 0 \leq x \leq 1 \\ T(0, t) = f(t), & 0 \leq t \leq 1 \\ T(x, 0) = 0, & 0 < x < 1 \\ T(1, t) = 0, & 0 \leq t \leq 1 \\ T(L_2, t) = g_2(t), & 0 \leq t \leq 1 \end{cases} \quad (2.34)$$

¹This MATLAB solver can be obtained from the author by the request on the following e-mail address: pingenda9@gmail.com

where we use $T(x, t)$ and $g_2(t)$ instead of $T^a(x, t)$ and $\widetilde{g}_2(t)$ just for simple notation. The problem (2.34) can be reformulated as linear discrete problem $Kf = g_2$, where K is the linear operator defined in Definition 2.3 which map the surface temperature $f(t)$ to another function of temperature measured at one location $x = L_2$, $g_2(t) = T(x = L_2, t)$ as shown in Fig.2.2. So for given equidistant grid domain $\Omega = \{0 = x_1 < x_2 \cdots < x_n = 1\}$ and time computational grid domain $\Omega' = \{0 = t_1 < t_2 \cdots < t_N = 1\}$, we then have discrete vectors $f = [f(t_1), f(t_2), \cdots, f(t_{N-1}), f(t_N)]^T$ and $g_2 = [g_2(t_1), g_2(t_2), \cdots, g_2(t_{N-1}), g_2(t_N)]^T$; thus the problem (2.34) is written as system of linear equation

$$Kf = g_2 \quad (2.35)$$

where K is $N \times N$ matrix, f and g_2 are $N \times 1$ vectors.

Lemma 2.3: *The matrix K can be obtained from the standard basis, $\{e_i\}$ of the space \mathbb{R}^N and shift invariance property, Proposition 2.2 of K .*

Proof: From (2.35), the vector f can be written as $f = \sum_{i=1}^N f(t_i)e_i$ then (2.35) becomes

$$K \left(\sum_{i=1}^N f(t_i)e_i \right) = \sum_{i=1}^N K(f(t_i)e_i) \quad (2.36)$$

$$\sum_{i=1}^N f(t_i)K(e_i) = g_2(t_i) \quad (2.37)$$

for $i = 1, 2, \cdots, N$ we can see that in order to evaluate the matrix-vector product Kf we need the vectors $K(e_i)$. Since $K(e_i) = K(:, i)$ then the above equation (2.37) can be written as system of equations

$$\left[K(:, 1), \cdots, K(:, N) \right] \begin{bmatrix} f(t_1) \\ \vdots \\ f(t_N) \end{bmatrix} = \begin{bmatrix} g_2(t_1) \\ \vdots \\ g_2(t_N) \end{bmatrix} \quad (2.38)$$

To obtain $K(:, 1)$ we first computed the temperature distribution $T(x, t)$ in the material by solving the *well-posed* problem corresponding to (2.34) by using the Crank-Nicolson scheme given in equation (2.33) for given boundary conditions $T(0, t) = e_1$, and $T(1, t) = 0$ where e_1 is the vector $[0, 1, 0, \cdots, 0]^T$ due to the initial condition $f(t = 0) = 0$. Therefore, we set $K(:, 1) = T(x = L_2, t)$ where $T(x = L_2, t)$ is the temperature calculated at the position $x = L_2$ from Crank-Nicolson scheme and in the same way for e_i we can compute each $K(:, i)$ for $i = 2, 3, \cdots, N$. But there is an efficient way to obtain the remaining column vectors of matrix K knowing only $K(:, 1)$ due the time shift invariant property of the linear operator K as follows:

Let $K(:, 1) = k = [k_1, k_2, \cdots, k_{N-1}, k_N]^T$ then the matrix K is given by

$$K_{i,j} = \begin{cases} k_{i-j+1}, & \text{if } i \geq j \\ 0, & \text{Otherwise} \end{cases}$$

that is

$$K = \begin{bmatrix} k_1 & 0 & 0 & 0 & \cdots & 0 \\ k_2 & k_1 & 0 & 0 & \cdots & 0 \\ k_3 & k_2 & k_1 & 0 & \cdots & 0 \\ \vdots & \vdots & \vdots & \ddots & \ddots & \vdots \\ k_{N-1} & k_{N-2} & k_{N-3} & \ddots & \ddots & 0 \\ k_N & k_{N-1} & k_{N-2} & \cdots & \cdots & k_1 \end{bmatrix} \quad (2.39)$$

and this matrix can be computed by using the developed MATLAB solver².

Definition 2.4: A matrix A is called Toeplitz if it is constant along diagonals, [22, 36].

According to Definition 2.4 the matrix K is lower triangular Toeplitz matrix, and the Fig.2.3 shows the time shift invariant property of matrix K by representing its first and twentieth column vectors.

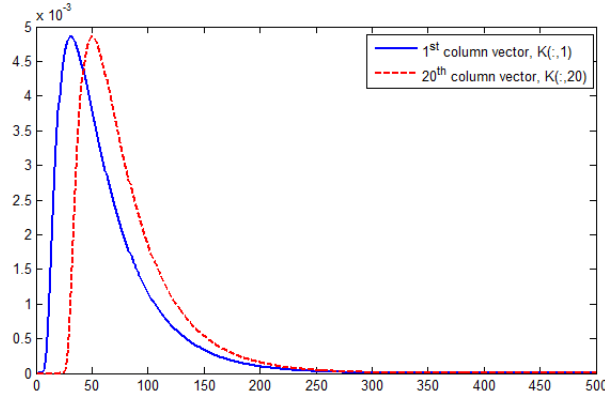


Fig. 2.3: First and twentieth column vectors of 500×500 matrix K

2.4 Regularization of the discrete problem

Suppose we want to solve for f from ill-posed problem (2.35) rewritten as $Kf = g_2^\delta$ where the exact data g_2 is not available but its noisy version, g_2^δ with

$$g_2^\delta = Kf + \eta \quad (2.40)$$

is available such that $\|g_2^\delta - g_2\| \leq \delta$, where η is normally distributed perturbation of variance δ representing error in the data with known noise level δ , and

$$\delta \stackrel{\text{def}}{=} \|\eta\| > 0. \quad (2.41)$$

²This MATLAB solver can be obtained from the author by the request on the following e-mail address: pingenda9@gmail.com

In the sense of Definition 1.1, if the operator K^{-1} is unbounded then $K^{-1}g_2^\delta$ is not good approximation of $K^{-1}g_2$ since K being ill-conditioned it will amplifies the errors in the solution; thus we need to replace the *ill posed-problem* by another *well posed problem* that involves a small parameter λ so that it can be solved in a stable way and its solution f_λ^δ tends to f of the original problem (2.35) as the noise level δ tends to zero for small regularization parameter λ , that process is defined as *regularization*. In other words, a regularization of K^{-1} is to replace the unbounded operator K^{-1} by a new bounded parameter-dependent family $\{R_\lambda\}$ of continuous operator and the best approximation of f is to set f_λ^δ to be $R_\lambda g_2^\delta$ which now can be computed in stable way since R_λ is bounded, as given in the following Definition 2.5.

Definition 2.5: (*Regularization*) Let $K: X \rightarrow Y$ be a bounded linear operator between the spaces X and Y , $\lambda_0 \in [0, +\infty)$. Now for every $\lambda \in (0, \lambda_0)$, let

$$R_\lambda : Y \rightarrow X$$

be a continuous(not necessary linear) operator. The family R_λ is called a regularization for K^{-1} , if for all g_2 belong in domain of K^{-1} , there exist a parameter choice rule $\lambda = \lambda(\delta, g_2^\delta)$ such that

$$\lim_{\delta \rightarrow 0} \sup \left\{ \left\| R_{\lambda(\delta, g_2^\delta)} g_2^\delta - K^{-1} g_2 \right\| \mid g_2^\delta \in Y, \left\| g_2^\delta - g_2 \right\| \leq \delta \right\} = 0 \quad (2.42)$$

holds. And $\lambda : \mathbb{R}^+ \times Y \rightarrow (0, \lambda_0)$ such that

$$\lim_{\delta \rightarrow 0} \sup \left\{ \lambda(\delta, g_2^\delta) \mid g_2^\delta \in Y, \left\| g_2^\delta - g_2 \right\| \leq \delta \right\} = 0 \quad (2.43)$$

For a specific g_2 belong in the domain of K^{-1} , a pair (R_λ, λ) is called a convergent regularization method for solving $Kf = g_2^\delta$ if equation (2.42) and (2.43) hold, [9].

Definition 2.6: (*Singular Value Decomposition(SVD)*) If K is $m \times n$ matrix, then there exist orthogonal matrices $U = (u_1, u_2, \dots, u_m) \in \mathbb{R}^{m \times m}$ and $V = (v_1, v_2, \dots, v_n) \in \mathbb{R}^{n \times n}$ such that $K = U \Sigma V^T$ with $\Sigma = \text{diag}(\sigma_1, \dots, \sigma_p) \in \mathbb{R}^{m \times n}$, $p = \text{rank}(K) \leq \min\{m, n\}$, where $\sigma_1 \geq \sigma_2 \geq \dots \geq \sigma_p \geq 0$.

Where σ_i are singular values of matrix K , u_i and v_i are left and right singular vectors of matrix K , respectively; such that $U^T = U^{-1}$ and $V^T = V^{-1}$, thus from that fact we have $K^{-1} = V \Sigma^{-1} U^T = V \text{diag}(\sigma_i^{-1}) U^T$, this can be found in [22] for example or any standard book on Linear Algebra for more details.

Corollary 2.1: If $K = U \Sigma V^T$ is the SVD of $K \in \mathbb{R}^{m \times n}$ and $m \geq n$, then for $i = 1, 2, \dots, n$ $K v_i = \sigma_i u_i$ and $K^T u_i = \sigma_i v_i$.

Now by using equation (2.40) and Definition 2.6 we can compute the approximation of $K^{-1}g_2^\delta$ as follows:

$$\begin{aligned}
K^{-1}g_2^\delta &= K^{-1}Kf + K^{-1}\eta \\
&= f + V \text{diag}(\sigma_i^{-1})U^T\eta \\
&= f + [v_1, \dots, v_n] \text{diag}(\sigma_1^{-1} \dots \sigma_n^{-1}) \begin{bmatrix} u_1^T \\ \vdots \\ u_n^T \end{bmatrix} \eta \\
&= f + v_1\sigma_1^{-1}u_1^T\eta + \dots + v_n\sigma_n^{-1}u_n^T\eta \\
&= f + \sum_{i=1}^n \sigma_i^{-1}(u_i^T\eta)v_i
\end{aligned}$$

We can see that

$$K^{-1}g_2^\delta = f + \sum_{i=1}^n \sigma_i^{-1}(u_i^T\eta)v_i \quad (2.44)$$

It is clear that $K^{-1}g_2^\delta$ is unstable, i.e., *ill-conditioned* due to the division of smaller singular values in equation (2.44), thus a more sophisticated approach is needed to handle that instability. Therefore, in [23] it was proposed that to deal with that instability we should multiply σ_i^{-1} in equation (2.44) by filtering function $\omega_\lambda(\sigma_i^2)$ such that $\omega_\lambda(\sigma_i^2)\sigma_i^{-1} \rightarrow 0$ as $\sigma \rightarrow 0$. And this yields the good approximation f_λ^δ of f given as

$$f_\lambda^\delta = \sum_{i=1}^n \omega_\lambda(\sigma_i^2)\sigma_i^{-1}(u_i^T g_2^\delta)v_i \quad (2.45)$$

And such regularizing filter function is

$$\omega_\lambda(\sigma_i^2) = \begin{cases} 1, & \text{if } \sigma_i^2 > \lambda \\ 0, & \text{if } \sigma_i^2 \leq \lambda \end{cases}$$

and then the equation (2.45) becomes

$$f_\lambda^\delta = \sum_{\sigma_i^2 > \lambda} \sigma_i^{-1}(u_i^T g_2^\delta)v_i$$

which is known as the *Truncated Singular Value Decomposition (TSVD)* solution of $Kf = g_2^\delta$ and this will filter away all singular components corresponding to smaller singular values, and another regularizing filter function is given by the equation (2.54) below.

2.4.1 Tikhonov regularization

In this part we look on the specific regularization method proposed by Tikhonov, see [24], where the Tikhonov regularization approach is to replace the ill-posed problem $K(f) = g_2^\delta$ by the more stable problem

$$\min_{f \in X} \left\{ \|Kf - g_2^\delta\|_2^2 + \lambda^2 \|f\|_2^2 \right\} \quad (2.46)$$

for given regularization parameter λ and also (2.46) is known as *Tikhonov functional*.

Proposition 2.3: : If K is $m \times n$ matrix, $m \geq n$ with $p = \text{rank}(K) \leq n$ and $K = U\Sigma V^T$ be the SVD of K . Then

(i) The unique minimizer of the Tikhonov functional (2.46) is the solution of the normal equation

$$(K^T K + \lambda^2 I_n) f = K^T g_2^\delta \quad (2.47)$$

where I_n is $n \times n$ identity matrix. Moreover, solving this normal equation is not ill-conditioned provided that λ is chosen appropriately.

(ii) The regularized solution of (2.35) where g_2 is not available but its noisy version g_2^δ is available, is given by the formula

$$f_\lambda^\delta = \sum_{i=1}^p \frac{\sigma_i(u_i^T g_2^\delta)}{\sigma_i^2 + \lambda^2} v_i \quad (2.48)$$

Proof: Let $\Phi(f) = \|Kf - g_2^\delta\|_2^2 + \lambda^2 \|f\|_2^2$, $r = Kf - g_2^\delta$ be the residual vector, h be arbitrary vector in \mathbb{R}^n and $\epsilon > 0$ be a small positive parameter. Then the minimizer of $\Phi(f)$ must satisfy

$$\frac{\partial}{\partial \epsilon} \Phi(f + \epsilon h)|_{\epsilon=0} = 0 \quad (2.49)$$

thus

$$\begin{aligned} \Phi(f + \epsilon h) &= \|K(f + \epsilon h) - g_2^\delta\|_2^2 + \lambda^2 \|(f + \epsilon h)\|_2^2 \\ &= \|r\|_2^2 + 2\epsilon \langle r, Kh \rangle + \epsilon^2 \|Kh\|_2^2 + \lambda^2 (\|f\|_2^2 + 2\epsilon \langle f, h \rangle + \epsilon^2 \|h\|_2^2) \end{aligned} \quad (2.50)$$

By using equation (2.50) and condition (2.49) we have

$$\begin{aligned} 2 \langle r, Kh \rangle + 2\lambda^2 \langle f, h \rangle &= 0 \\ \iff \langle K^T r, h \rangle + \lambda^2 \langle f, h \rangle &= 0 \\ \iff \langle K^T r + \lambda^2 f, h \rangle &= 0 \end{aligned} \quad (2.51)$$

Since h is arbitrary, it follows from the equation (2.51) that $K^T r + \lambda^2 f = 0$, then

$$\begin{aligned} K^T(Kf - g_2^\delta) + \lambda^2 f &= 0 \\ \iff K^T K f + \lambda^2 f &= K^T g_2^\delta \\ \iff (K^T K + \lambda^2 I_n) f &= K^T g_2^\delta \end{aligned} \quad (2.52)$$

Hence the proof of (i) in equation (2.52). It follows also that f_λ^δ is given by

$$f_\lambda^\delta = R_\lambda g_2^\delta \quad (2.53)$$

where $R_\lambda = (K^T K + \lambda^2 I_n)^{-1} K^T$. Using $K = U \Sigma V^T$, we have

$$\begin{aligned} R_\lambda &= (V \Sigma^2 V^T + \lambda^2 V I_n V^T)^{-1} V \Sigma U^T \\ &= [V (\Sigma^2 + \lambda^2 I_n) V^T]^{-1} V \Sigma U^T \\ &= V (\Sigma^2 + \lambda^2 I_n)^{-1} V^T V \Sigma U^T \\ &= \sum_{i=1}^p \left(\frac{\sigma_i^2}{\sigma_i^2 + \lambda^2} \frac{1}{\sigma_i} \right) u_i^T v_i \end{aligned}$$

By inspection it is clear that $R_\lambda \rightarrow K^{-1}$ as $\lambda \rightarrow 0$. Therefore, from (2.53) it follows that

$$\begin{aligned} f_\lambda^\delta &= R_\lambda g_2^\delta = \sum_{i=1}^p \left(\frac{\sigma_i^2}{\sigma_i^2 + \lambda^2} \frac{1}{\sigma_i} \right) (u_i^T g_2^\delta) v_i \\ &= \sum_{i=1}^p \frac{\sigma_i (u_i^T g_2^\delta)}{\sigma_i^2 + \lambda^2} v_i \end{aligned}$$

Moreover, the regularized solution f_λ^δ given in (2.48) can be obtained by multiplying the equation (2.45) with the regularization filter function known as *Tikhonov filter function*, [23]

$$\omega_\lambda(\sigma_i^2) = \frac{\sigma_i^2}{\sigma_i^2 + \lambda^2} \quad (2.54)$$

to dump out the smaller singular values in equation (2.45).

Proposition 2.4: *The application of Tikhonov filter function $\omega_\lambda(\sigma_i^2)$ to σ_i^{-1} , $\omega_\lambda(\sigma_i^2)\sigma_i^{-1}$ is bounded by λ^{-1} .*

Proof: For fixed σ

$$\omega_\lambda(\sigma^2)\sigma^{-1} = \frac{1}{\sigma + \frac{\lambda^2}{\sigma}} \quad (2.55)$$

now here we consider two cases where $\sigma^2 > \lambda^2$ and $\sigma^2 \leq \lambda^2$ and we have the following the following:

1. *First case:* For $\sigma^2 > \lambda^2$ we have $\sigma > \lambda$ since σ and λ are positive numbers then $\sigma + \frac{\lambda^2}{\sigma} > \lambda$ and from (2.55) we have

$$\omega_\lambda(\sigma^2)\sigma^{-1} = \frac{1}{\sigma + \frac{\lambda^2}{\sigma}} < \frac{1}{\lambda} \quad (2.56)$$

2. *Second case:* For $\sigma^2 \leq \lambda^2$ we have $\sigma \leq \lambda$, since σ and λ are positive numbers then $\sigma + \frac{\lambda^2}{\sigma} \geq \lambda$, and also from (2.55) we have:

$$\omega_\lambda(\sigma^2)\sigma^{-1} = \frac{1}{\sigma + \frac{\lambda^2}{\sigma}} \leq \frac{1}{\lambda} \quad (2.57)$$

Therefore, from (2.56) and (2.57) we conclude that $\omega_\lambda(\sigma^2)\sigma^{-1} \leq \lambda^{-1}$.

Remark 2.3: When we have a-priori information about the solution of inverse problem, the equation (2.46) becomes

$$\min_{f \in X} \left\{ \|Kf - g_2^\delta\|_2^2 + \lambda^2 \|Lf\|_2^2 \right\} \quad (2.58)$$

where L is a discretized differential $n \times n$ operator.

Therefore, (2.58) is known as **generalized Tikhonov regularization** form of the problem $K(f) = g_2^\delta$, [22, 23].

2.4.2 Parameter choice rule

From the Definition 2.5 we have seen that the family $\{R_\lambda\}$ of continuous operator should be chosen such that $\|R_{\lambda(\delta, g_2^\delta)} g_2^\delta - K^{-1} g_2\| \rightarrow 0$ as $\|g_2^\delta - g_2\| \leq \delta \rightarrow 0$ that is $f_\lambda^\delta = R_\lambda g_2^\delta \rightarrow f = K^{-1} g_2$. Intuitively, as the noise level δ tends to zero more information present in g_2^δ can be considered reliable, and should be used. Therefore the rule for selecting regularization parameter λ should depend on δ and possibly on g_2^δ . Hence the following definition:

Definition 2.7: If the regularization parameter λ depends only the noise level, i.e, $\lambda = \lambda(\delta)$ then $\lambda(\delta)$ is called a-priori parameter choice rule. While, if the regularization parameter λ depend on noise level δ and the noisy data g_2^δ , i.e, $\lambda = \lambda(\delta, g_2^\delta)$ then $\lambda(\delta, g_2^\delta)$ is called a-posteriori parameter choice rule.

In fact, the regularization parameter λ should be chosen such that we are guaranteed that regularized solution error E_λ , i.e, sum of the solution truncation error due to regularization E_λ^{trunc} , and the noise amplification error E_λ^{noise} converge to zero as the noise level δ tends to zero, [23]. By definition, the regularized solution error is given as

$$E_\lambda \stackrel{\text{def}}{=} f_\lambda^\delta - f \quad (2.59)$$

Now, using equation (2.40) and (2.45) and Corollary 2.1 we have the following

$$\begin{aligned} E_\lambda &= \sum_{i=1}^n \omega_\lambda(\sigma_i^2) \sigma_i^{-1} \sigma_i v_i^T f - (v_i^T f) v_i + \sum_{i=1}^n \omega_\lambda(\sigma_i^2) \sigma_i^{-1} (u_i^T \eta) v_i \\ &= \sum_{i=1}^n (\omega_\lambda(\sigma_i^2) - 1) (v_i^T f) v_i + \sum_{i=1}^n \omega_\lambda(\sigma_i^2) \sigma_i^{-1} (u_i^T \eta) v_i \\ &= E_\lambda^{trunc} + E_\lambda^{noise} \end{aligned}$$

where

$$E_\lambda^{trunc} = \sum_{i=1}^n (\omega_\lambda(\sigma_i^2) - 1) (v_i^T f) v_i \quad (2.60)$$

$$E_\lambda^{noise} = \sum_{i=1}^n \omega_\lambda(\sigma_i^2) \sigma_i^{-1} (u_i^T \eta) v_i \quad (2.61)$$

Since for any fixed σ the Tikhonov filter function given in (2.54) tends to 1 as λ tends 0 then we can conclude from (2.60) that the solution truncation error E_λ^{trunc} due to regularization goes to zero as regularization parameter λ goes to zero, that is

$$E_\lambda^{trunc} \longrightarrow 0 \text{ as } \lambda \longrightarrow 0. \quad (2.62)$$

Furthermore, using equation (2.41) and Proposition 2.4 we can see that the noise amplification error defined in (2.61) is bounded by $\lambda^{-1}\delta$ as follows: From (2.61) we have

$$\begin{aligned} \|E_\lambda^{noise}\|_2^2 &\leq \max(\omega_\lambda(\sigma_i^2)\sigma_i^{-1})^2 \sum_{i=1}^n (u_i^T \eta)^2 \\ &\leq (\lambda^{-1})^2 \|\eta\|_2^2 = \lambda^{-2}\delta^2 \end{aligned}$$

Thus, we have $\|E_\lambda^{noise}\|_2 \leq \lambda^{-1}\delta$. Therefore, if we choose $\lambda = \delta^p$ with $0 < p < 1$ then $\|E_\lambda^{noise}\|_2 \longrightarrow 0$ as $\delta \longrightarrow 0$. Hence, one can have the following regularization priori parameter choice rule

$$\lambda = \lambda(\delta) = \delta^p, \quad 0 < p < 1 \quad (2.63)$$

that will guarantee that $E_\lambda \longrightarrow 0$ as $\delta \longrightarrow 0$ since $E_\lambda^{trunc} + E_\lambda^{noise}$. However, there is a-posteriori parameter choice rule that has attained a widespread interest in the literature, for instance in [9, 23, 25, 37], that is the *discrepancy principle* due to Morozov [38] where the regularization parameter depends on both $\|Kf_\lambda^\delta - g_2^\delta\|_2$ and the noise level, δ ; that is

$$\lambda = \lambda(\delta, g_2^\delta) := \sup \{ \lambda > 0 \mid \|Kf_\lambda^\delta - g_2^\delta\|_2 \leq \delta \} \quad (2.64)$$

In addition, another a-posteriori parameter choice rule so-called *L-curve criterion* was advocated by Hansen, see [25, 39, 40], it consists of plotting in a double logarithmic scale the norm or semi-norm $\|f_\lambda^\delta\|_2$ of the regularized solutions versus the residuals norm $\|Kf_\lambda^\delta - g_2^\delta\|_2$ in which its graph is typically looks like the shape of the letter *L* as shown in the Fig.2.4, and the method has been used for instance in [9, 23, 37].

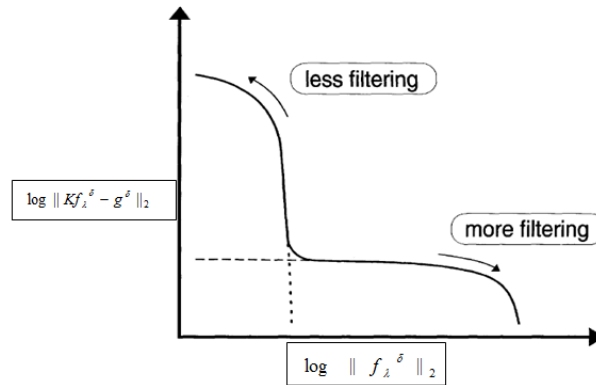


Fig. 2.4: The generic form of L-curve, adopted from [25]

The important feature basis for the L-curve criterion for choosing the regularization parameter, was proposed in [37, 39, 40] that a point on the graph near the corner of the L-curve represents a reasonable compromise between minimization of $\|f_\lambda^\delta\|_2$ and $\|Kf_\lambda^\delta - g_2^\delta\|_2$ and hence the good regularization parameter λ is one that corresponds to a regularized solution near the "corner" of the L-curve since in that region we achieve a small residual norm and keeping the solution semi-norm reasonably small, i.e, we are looking a fair balance in keeping both of these values small as possible; as well the algorithm for finding out the corner point of L-curve was developed, see [37, 40].

Furthermore, for more details about L-curve method for analysis of discrete ill-posed problems, especially the convergence properties of L-curve regularization parameter selection and its limitations, we refer to [41, 42] for the case of Tikhonov regularization.

2.4.3 Numerical experiments

In this part three numerical experiments are presented in order to illustrate the usefulness of the Tikhonov regularization theory presented in Section 2.4.1 and the test problems have been solved using MATLAB software³. The tests were constructed in the following way: First we have selected boundary data $T(0, t) = f(t)$ and $T(1, t) = 0$ for $0 \leq t \leq 1$, and calculate the data vector $g = T(x = L_2, t)$ by solving a well-posed boundary value problem (2.34) on the interval $0 \leq x \leq 1$, using the Crank-Nicolson implicit scheme as described in Section 2.2, then we added a normally distributed perturbation η to data vector g to obtain the noise data vector $g^\delta = g + \delta * \eta$ to be used in estimation of surface temperature f from $Kf = g^\delta$, where K is 1000×1000 matrix obtained using Lemma 2.3 and description given in equations (2.36-2.39), f and g^δ are 1000×1 vectors for all the following test problems Test 1, 2, and 3. Besides, the regularization parameters used were chosen according the L-curve criterion presented in *Fig.2.4*.

Test 1: The problem (2.34) was solved using $T(0, t) = f(t)$ shown in *Fig.2.5(a)* as the exact solution with variable coefficient function,

$$a(x) = 1 + 0.3 \cos(x^2); \quad 0 \leq x \leq 1 \quad (2.65)$$

Also we used the data vector g^δ shown in *Fig.2.5(b)* whose length of 1000 which included a normally distributed perturbation of variance $\delta = 10^{-3}$. The results from this test are shown in *Fig.2.9(b)*.

Test 2: We solved the problem (2.34) using the function $T(0, t) = f(t)$ shown in *Fig.2.6(a)* as the exact solution with variable coefficient,

$$a(x) = 1 + (1 - x^2), \quad 0 \leq x \leq 1 \quad (2.66)$$

³The MATLAB solver used in numerical computation can be obtained from the author by the request on the following e-mail address: pingenda9@gmail.com

and the data vector $g = T(0.8, t)$ whose length of 1000 which included a normally distributed perturbation of variance of $8 * 10^{-4}$ shown in *Fig.2.6(b)* was used. The results from the test are presented in *Fig.2.9(d)*.

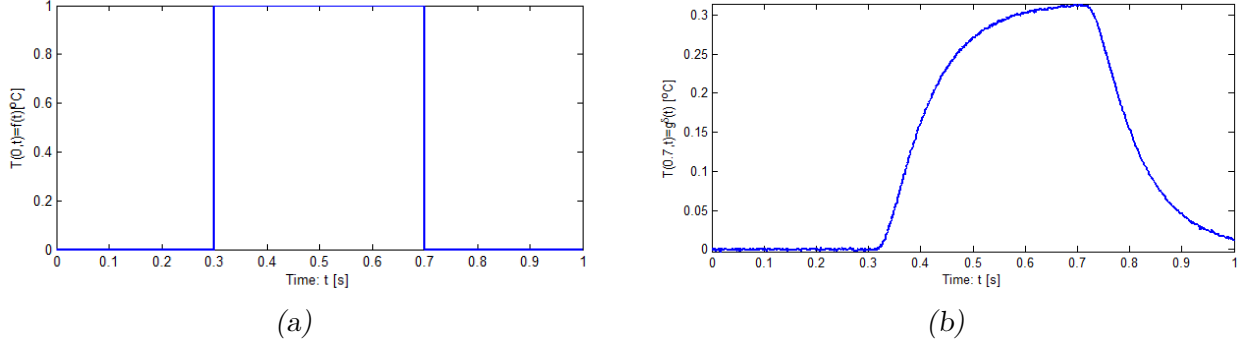


Fig. 2.5: The left subplot is the exact solution data function $T(0,t) = f(t)$ with $0 \leq t \leq 1$, and the right subplot is its corresponding noisy data vector $T(0.7,t) = g(t)$ which added some noise data with noise level $\delta = 10^{-3}$.

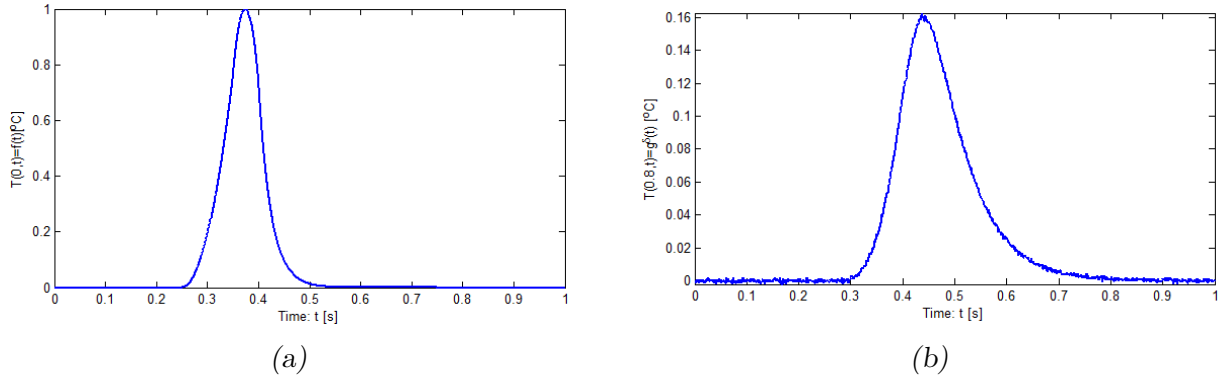


Fig. 2.6: The left subplot is the exact solution data function $T(0,t) = f(t)$ with $0 \leq t \leq 1$ and the right subplot is its corresponding noisy data vector $T(0.8,t) = g(t)$ which added some noise data with noise level $\delta = 8 * 10^{-4}$.

Test 3: The problem (2.34) was solved using $T(0, t) = f(t)$ shown in *Fig.2.7(a)* as the exact solution with variable coefficient

$$a(x) = 0.5 + 0.5(1 - \cos(x))^2, \quad 0 \leq x \leq 1 \quad (2.67)$$

with the data vector $g = T(0.3, t)$ whose length of 1000 which added a normally distributed perturbation of variance of 10^{-3} displayed in *Fig.2.7(b)* and the the results from the test are given in *Fig.2.9(f)*.

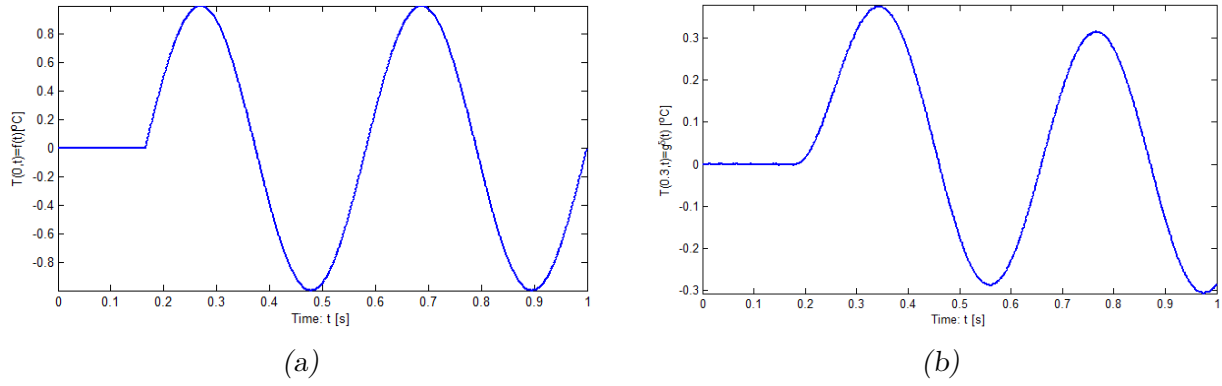


Fig. 2.7: The left subplot is the exact solution data function $T(0,t) = f(t)$; $0 \leq t \leq 1$ with oscillation frequency of 4π and the right subplot is its corresponding noisy data vector $g = T(0.3,t)$ which added some noise data with noise level $\delta = 10^{-3}$.

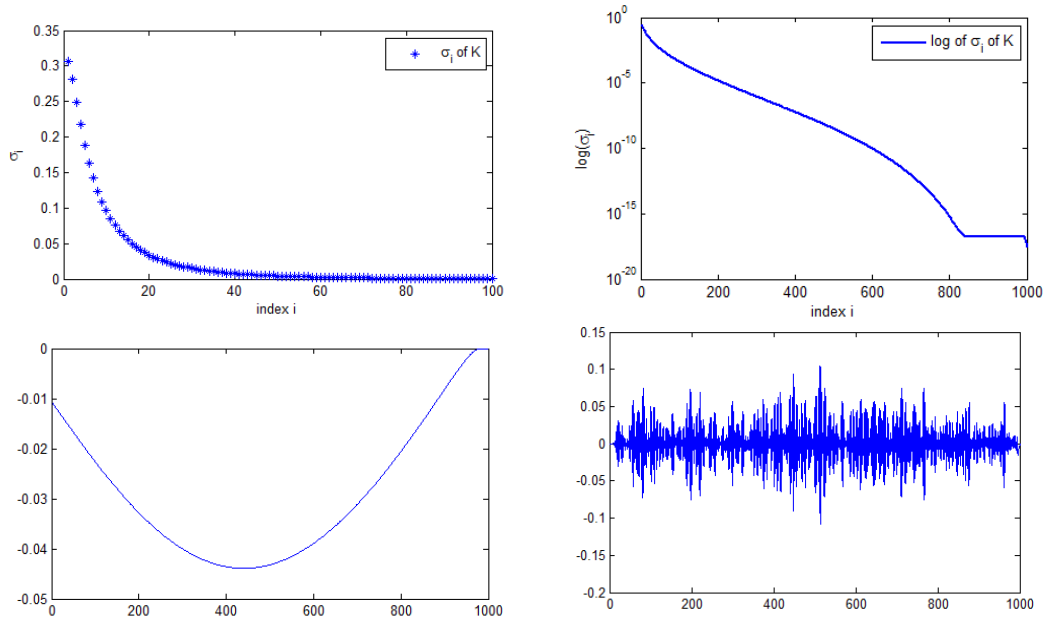


Fig. 2.8: The left top subplot shows the distribution of singular values σ_i of matrix K and the right top subplot is semilogy plot of singular values of matrix K , the bottom left and right subplots are right singular vectors v_1 and v_{1000} corresponding to largest singular value σ_1 and smallest singular value σ_{1000} of matrix K respectively.

The Fig.2.8 represents graphically the distribution of singular values σ_i of matrix K from Test 1 and it is clear that they are decaying gradually to zero which result in high condition number $\kappa(K) = 1.1593e + 17$ and also we can see that the right singular vectors of matrix K have more sign changes in their elements as the σ_i decreases, then the problem of computing f from $Kf = g^\delta$ is an *ill-posed* and regularization is needed. Furthermore, the test problems Test 2 and Test 3 are *ill-posed*.

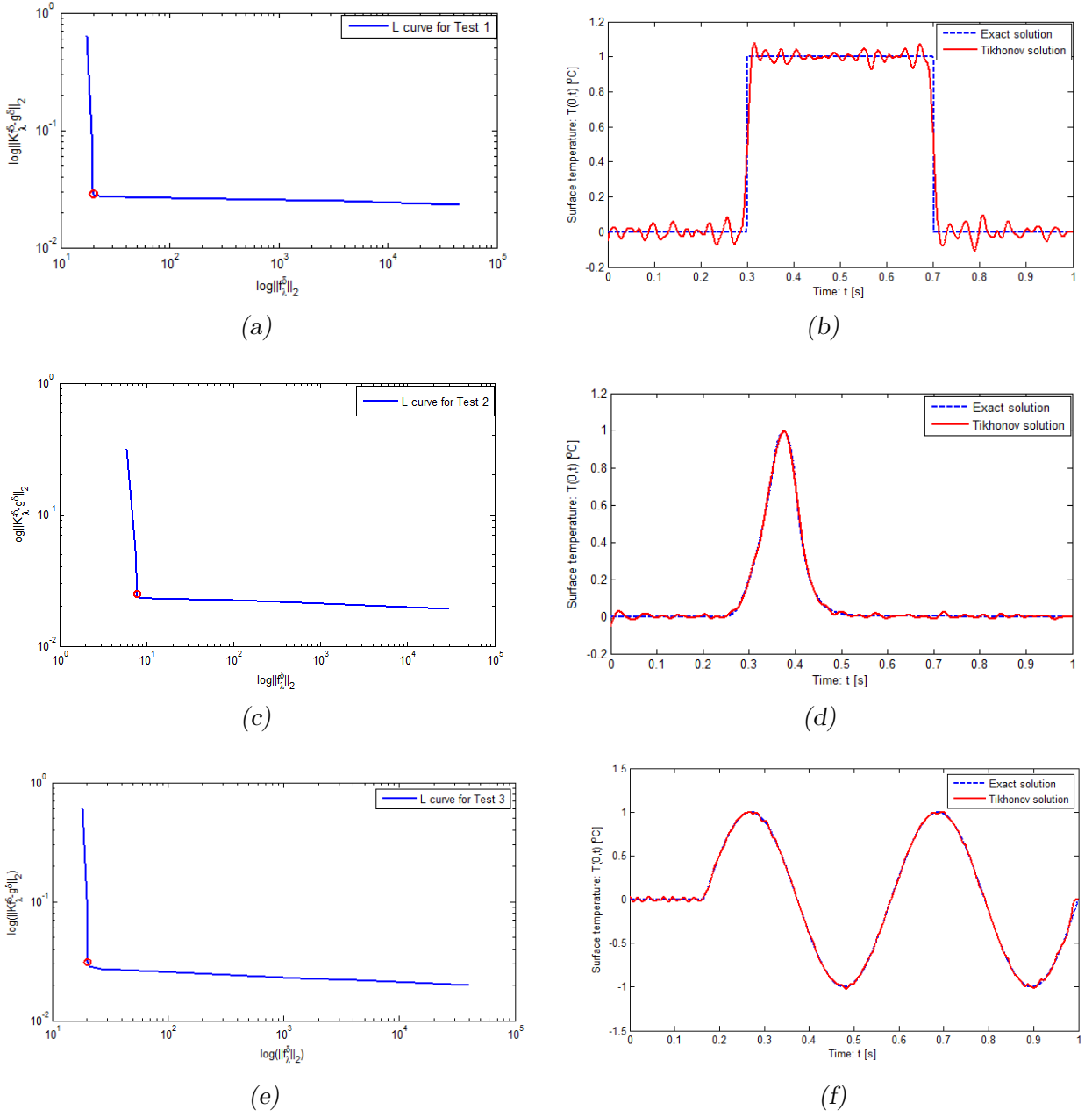


Fig. 2.9: The top, middle and bottom left subplots show respectively the L curves for test problems Test 1, Test 2, and Test 3. And also the top, middle, and bottom right subplot show the regularized solution (solid-line) for Test 1, Test 2, and Test 3 with regularization parameters $\lambda = 0.0032$, 0.0100 , and 0.0100 respectively obtained from L-curve analysis, and also the exact solution(dashed-line) are displayed for each test problem.

2.5 Extension to multiple measurements

In this section we seek to improve the accuracy of the solution of the test problem *Test 1* shown in *Fig.2.9(b)* and stability of the inverse problem by include more additional data in estimation of surface temperature as follows: we solved the well posed problem (2.34) using Crank-Nicolson implicit scheme with some given $T(0, t) = f(t)$ and $T(1, t) = 0$ as boundary

conditions to find the temperature distribution $T(x, t)$ inside the material and thereafter the temperature measured at location $x = L_i$, $T(L_i, t) = g_i(t)$ with $0 < L_i < 1$ for $i = 1, 2, \dots, m$ as shown in Fig.2.10 were used in estimation of surface temperature $T(0, t) = f(t)$ from the problem (2.1), that is for m measurement points we have $g(t) = (g_1(t), \dots, g_m(t))$.

For given equidistant grid domain $\Omega = \{0 = x_1 < x_2 < \dots < x_n = 1\}$ and time computational grid domain $\Omega' = \{0 = t_1 < t_2 < \dots < t_N = 1\}$, we have $f = [f(t_1), f(t_2), f(t_3), \dots, f(t_N)]^T$ and $g = [(g_1(t_1), \dots, g_1(t_N)), \dots, (g_m(t_1), \dots, g_m(t_N))]^T$ and thus the problem (2.34) can be written as system of linear equation $Kf = g$ where f and g are $N \times 1$, $m \times N \times 1$ vectors, respectively and K is the operator defined in Definition 2.8 below.

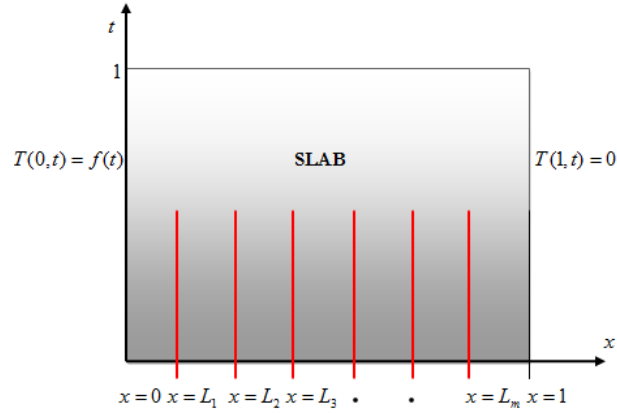


Fig. 2.10: Measurement points inside the material

Definition 2.8: We define the operator $K : C^0([0, 1]) \rightarrow (C^0([0, 1]))^m$ that maps $f(t)$ to $g(t) = (g_1(t), g_2(t), \dots, g_m(t))$ with $g_i(t) = T(L_i, t)$ for $i = 1, \dots, m$ where $T(x, t)$ satisfies the problem (2.34) and $0 < L_i < 1$, that is $(Kf)(t) = g(t)$. Where f and g are continuous functions over $[0, 1]$, and $(C^0([0, 1]))^m$ is the product space of m $C^0([0, 1])$.

Remark 2.4: The operator K defined in Definition 2.8 satisfies the Lemma 2.2, Proposition 2.1 and Proposition 2.2. That is the operator is linear, there exist unique $T(L_i, t)$ and the operator is shift invariant in time.

Thus, for each $i = 1, \dots, m$ and $j = 1, \dots, N$ the problem (2.34) is written as

$$K_i f(t_j) = g_i(t_j) \tag{2.68}$$

where f and g_i are $N \times 1$ vectors and K_i is $N \times N$ matrix obtained by using Lemma 2.4 and Proposition 2.2 for each measurement point $x = L_i$.

Lemma 2.4: Matrix K_i is lower triangular Teoptiz, and it can be obtained from the standard basis, $\{e_j\}$ of the space \mathbb{R}^N and shift invariance property, Proposition 2.2.

Proof: We write f as $f = \sum_{j=1}^N f(t_j)e_j$ then 2.68 becomes

$$K_i \left(\sum_{j=1}^N f(t_j)e_j \right) = g_i(t_j) \quad (2.69)$$

$$\sum_{j=1}^N K_j (f(t_j)e_j) = g_i(t_j) \quad (2.70)$$

$$\sum_{j=1}^N f(t_j)K_i(e_j) = g_i(t_j) \quad (2.71)$$

Since $K_i(e_j) = K_i(:, j)$ then the equation 2.71 can be written as system of equation

$$\left[K_i(:, 1), \dots, K_i(:, N) \right] \begin{bmatrix} f(t_1) \\ \vdots \\ f(t_N) \end{bmatrix} = \begin{bmatrix} g_i(t_1) \\ \vdots \\ g_i(t_N) \end{bmatrix}$$

where $K_i(:, 1)$ is $T(x = L_i, t)$ with $T(x, t)$ is the solution of the well posed problem (2.34) obtained using Crank-Nicolson implicit scheme with $T(0, t) = e_1$ and $T(1, t) = 0$ as boundary conditions where $e_1 = [0, 1, 0, \dots, 0]^T$; and then due the shift invariant property, for obtained $K_i(:, 1) = [k_1, k_2, \dots, k_N]^T$ we have

$$K_i = \begin{bmatrix} k_1 & 0 & 0 & 0 & \dots & 0 \\ k_2 & k_1 & 0 & 0 & \dots & 0 \\ k_3 & k_2 & k_1 & 0 & \dots & 0 \\ \vdots & \vdots & \vdots & \ddots & \ddots & \vdots \\ k_{N-1} & k_{N-2} & k_{N-3} & \ddots & \ddots & 0 \\ k_N & k_{N-1} & k_{N-2} & \dots & \dots & k_1 \end{bmatrix} \quad (2.72)$$

that can be computed by using the same solver² as for matrix given (2.39). Therefore, for m measurement points the operator K defined in Definition 2.8 is $m * N \times N$ matrix written as

$$K = [K_1; K_2; \dots; K_m] \quad (2.73)$$

such that $Kf = g$, where f and g are $N \times 1$, $m * N \times 1$ vectors.

2.5.1 Numerical experiments

Test 4: The well posed problem (2.34) was solved using $T(0, t) = f(t)$ shown in *Fig.2.5(a)* as the exact solution with the same variable coefficient function as in (2.65) to have the temperature distribution $T(x, t)$ inside the material. In addition, to improve the accuracy of the solution for one measurement presented in *Fig.2.9(b)* and stability of the inverse problem, two additional measurement points, $x = 0.5$, and $x = 0.6$ were used to create the data vector $g = [T(x = 0.5, t), T(x = 0.6, t), T(x = 0.7, t)]^T$ whose length of 3000 and added some

normally distributed perturbation of variance $\delta = 10^{-3}$ to have the data vector with noise g^δ to be used in recovering f from discrete linear problem $Kf = g^\delta$; where $K = [K_1; K_2; K_3]$ is 3000×1000 matrix that is computed based on Lemma 2.4 and equation (2.73) with K_1 , K_2 , and K_3 are matrices corresponding to the measurement $x = 0.5, 0.6$, and 0.7 , respectively as it was described from equations (2.68-2.72). The computational results ³ are presented in Fig.2.12(b).

Moreover, the singular values and some singular vectors are represented graphically in Fig.2.11 which shows that the singular values σ_i of matrix K resulting from three measurement points are also decaying gradually to zero which result in high condition number $\kappa(K) = 3.0778e+16$ and both singular vectors of K have more sign changes in their elements as the σ_i tend to zero; then the problem of computing f from $Kf = g^\delta$ is an *ill-posed* and thus the regularization is needed.

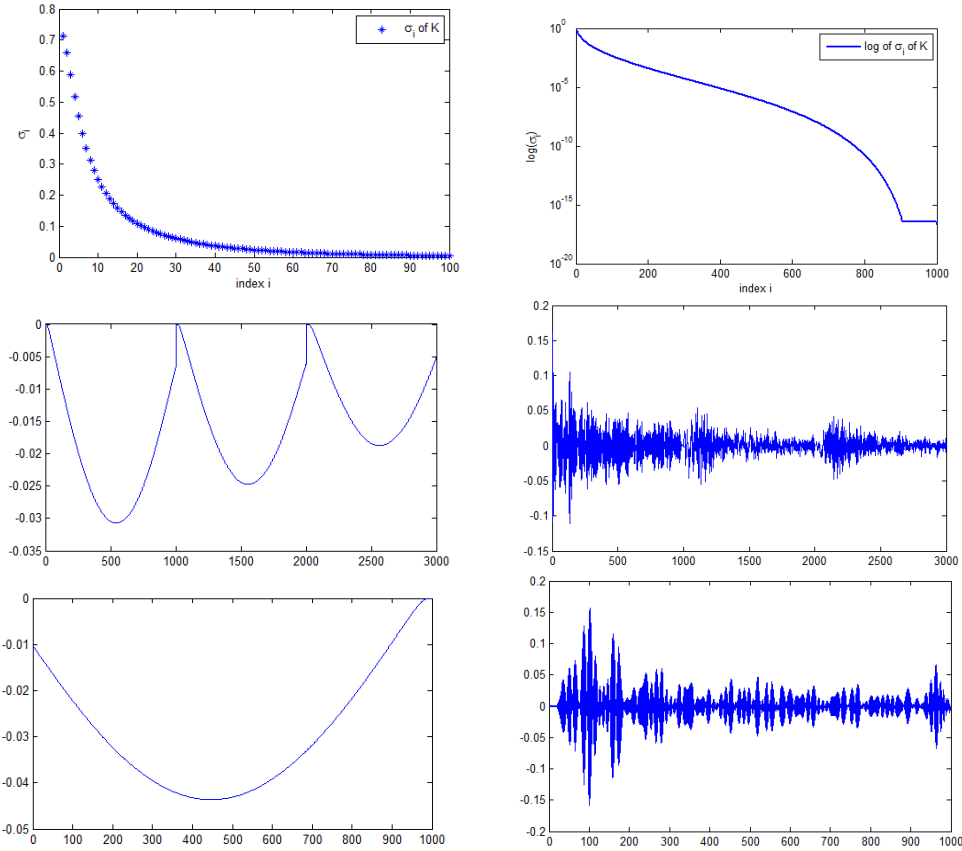


Fig. 2.11: The left top subplot shows the distribution of singular values σ_i of matrix K and the right top subplot is semilogy plot of singular values of matrix K , the middle left and right subplots are left singular vectors u_1 and u_{1000} corresponding to largest singular value σ_1 and σ_{1000} of matrix K , and the bottom left and right subplots are right singular vectors v_1 and v_{1000} corresponding to largest singular value σ_1 and smallest singular value σ_{1000} of matrix K respectively.

Even though the test problem Test 4 is *ill-posed*, it is more stable than the test problem Test 1 since the corresponding matrix K has small condition number $\kappa(K) = 3.0778e+16$

comparing to the test problem Test 1 for one measurement point whose its corresponding matrix K has condition number $\kappa(K) = 1.1593e + 17$.

Test 5: We solved the problem (2.34) using $T(0, t) = f(t)$ shown in *Fig.2.5(a)* as the exact solution with the same variable coefficient function as in (2.65) and also five measurement points, $x = 0.8, 0.85, 0.9, 0.95,$ and 1 were used to create the data vector $g = [T(x = 0.8, t), T(x = 0.85, t), T(x = 0.9, t), T(x = 0.95, t), T(x = 1, t) = 0]^T$ whose length of 5000 and added some normally distributed perturbation of variance $\delta = 10^{-3}$ to obtain noisy data vector g^δ to be used in estimation f from discrete linear problem $Kf = g^\delta$; where $K = [K_1; K_2; K_3; K_4; K_5]$ is 5000×1000 matrix that is computed based on Lemma 2.4 and equation (2.73) with K_1, \dots, K_5 are matrices corresponding to the measurement points $x = 0.8, 0.85, 0.9, 0.95$ and 1 , respectively as it was described from equations (2.68-2.72). The computational results³ are shown in *Fig.2.12(d)*.

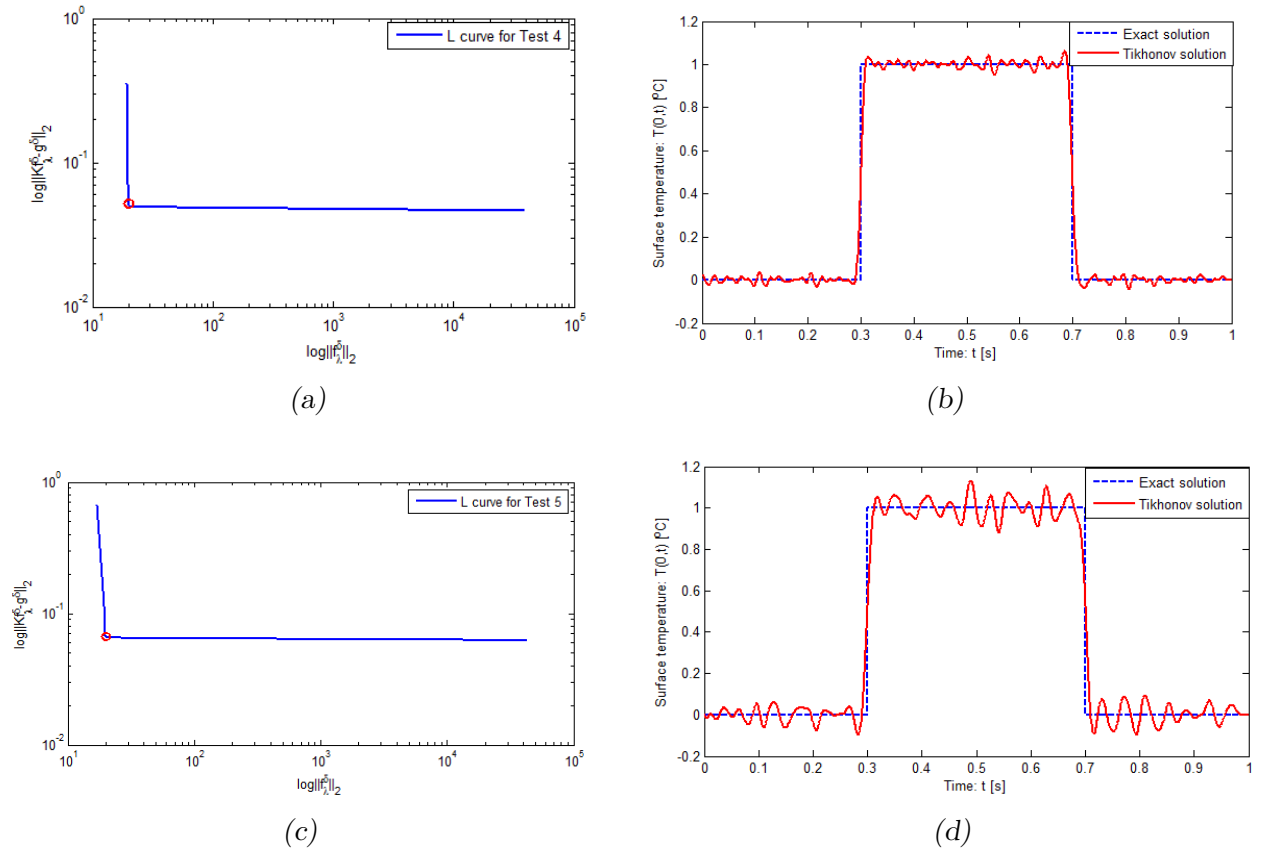


Fig. 2.12: The top, and bottom left subplots show respectively the L-curves for test problems Test 4, and Test 5 whose corresponding matrix K has condition number, $\kappa(K) = 6.6248e + 16$. And also the top, and bottom right subplots show the regularized solution (solid-line) for Test 4, and Test 5 with regularization parameters, $\lambda = 0.0100,$ and 0.0032 respectively obtained from L-curve analysis, and also the exact solution(dashed-line) are displayed for each test problem.

Furthermore, more measurement points were included in the experiment to investigate the impact of using the additional data on the estimate of the surface temperature and the sta-

bility of the inverse problem. The results shown in *Fig.2.13* are the norm of the solution errors, $\|f - f_\lambda^\delta\|_2$ and the residuals norm, $\|Kf_\lambda^\delta - g^\delta\|_2$ from nine experiments, where different number of measurement points were taken into consideration, the results reveal that the more you include more data the more the solution errors goes to zero, see *Fig.2.13(a)* and hence the more the problem is stable, and also the residuals tends to zero as the regularization parameter λ tends to zero, see *Fig.2.13(b)*.

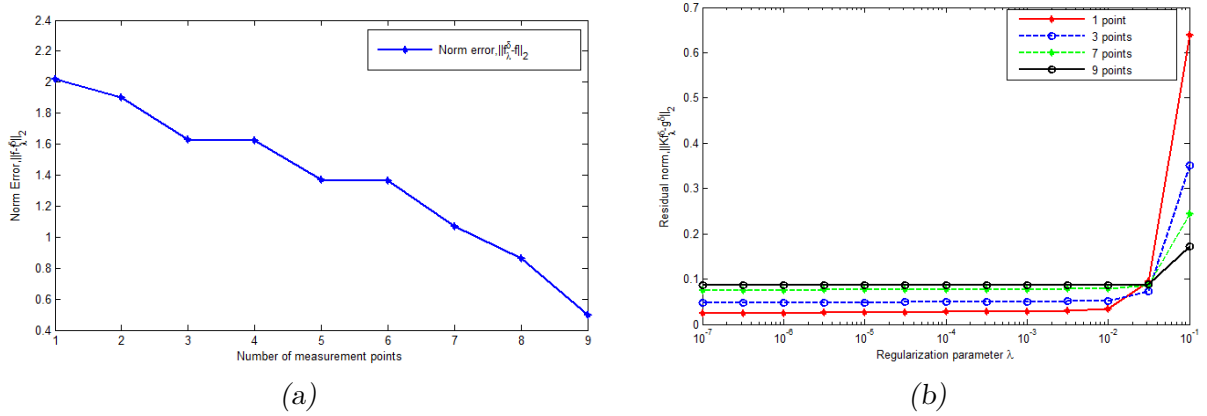
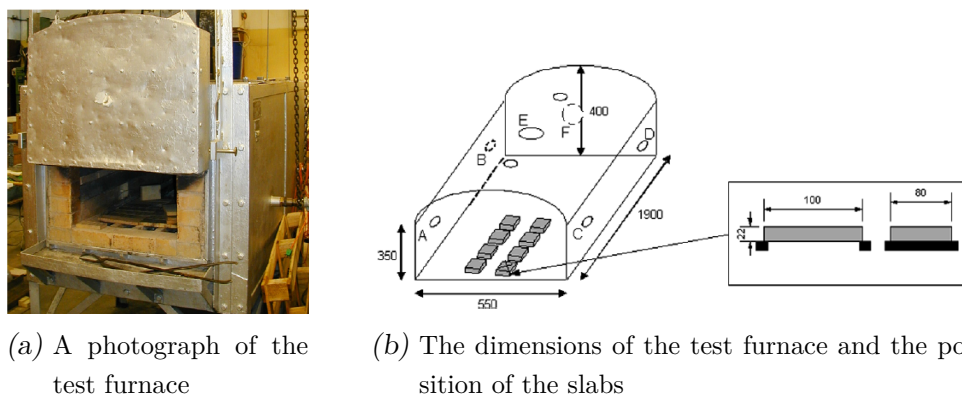


Fig. 2.13: The left subplot shows the distribution of error between the exact and regularized solutions, $\|f_\lambda^\delta - f\|_2$ from different nine numerical experiments, and right subplot shows the semilogx of residuals, $\|Kf_\lambda^\delta - g^\delta\|_2$ and against regularization parameter, λ for different measurement points used in estimation of surface temperature, $T(x=0, t) = f(t)$.

3. TEMPERATURE ESTIMATION ON A STEEL SURFACE

In this chapter we present an example from an industrial problem where the regularization method presented in previous chapter is used to investigate the usefulness of an inverse method to compute the surface temperature in a high temperature heating application. The usefulness of the method is demonstrated by using the exact data of measured temperatures during an experiment which was conducted and presented in [12].

3.1 Experimental setup



(a) A photograph of the test furnace

(b) The dimensions of the test furnace and the position of the slabs

Fig. 3.1: Test furnace and its dimensions, adopted from [12]

A fuel fired test furnace and its dimensions used in experiment and the total of eight steel slabs initially at $25^{\circ}C$ with dimensions $100 \times 80 \times 22mm$ were heated in the test furnace shown in Fig.3.1(a) where the temperature was approximately $1250^{\circ}C$ with total inner volume of $0.39m^3$, and also the composition of the material of the steel slabs used are shown Tab 3.1. In addition, the furnace was equipped with a burner that produces heat at position F and thermocouples at positions A , B , C , D and E respectively, see Fig.3.1(b). Lastly, to take the measurements of the flue gas composition, the gas analyzers were also positioned at acceptable positions. The maximum allowed heat density in the furnace was $200kW/m^3$ which allowed for a burner capacity of $78kW$.

Moreover, to be able to read the temperature histories that were recorded by data acquisition system, three thermocouples $TC1$, $TC2$, and $TC3$ were installed under the surface, i.e $x = 0$ at positions $x = x_1$, $x = x_2$ and $x = x_3$ respectively in the center of the slab that is pointed, see Fig.3.1(b) along the x -axis orthogonal to the top surface as shown in Fig.3.2.

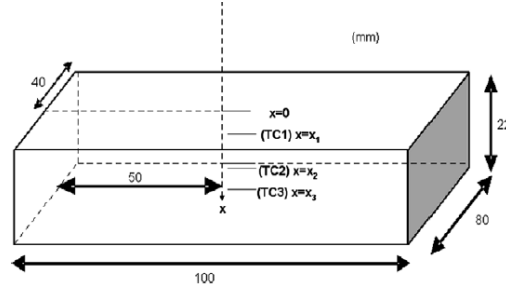


Fig. 3.2: The dimensions of the test slab equipped with thermocouples. The surface of the slab is positioned at $x = 0$, adopted from [12]

Tab. 3.1: The composition of the steel used for these investigations, adopted from [12]

Element	C	Si	Mn	S	P	Cr	Ni	Mo	Cu	Al
Wt.%	0.06	0.01	0.38	0.035	0.017	0.022	0.055	0.030	0.08	0.001

3.2 Data and computational results

The industrial experiment presented in this thesis, thermocouples $TC1$, $TC2$, and $TC3$ were positioned at locations $x_1 = 5\text{mm}$, $x_2 = 25\text{mm}$ and $x_3 = 45\text{mm}$ below the surface and those thermocouples gave the temperature histories $g_{i=1,2,3}(t)$, see Fig3.3(a), for $0 \leq t \leq 93.7\text{s}$, and the sampled data vectors of length 937 of the measured temperature histories at those locations are displayed in Fig.3.3(b) where the time interval $[0, 93.7]$ was scaled to $[0, 1]$.

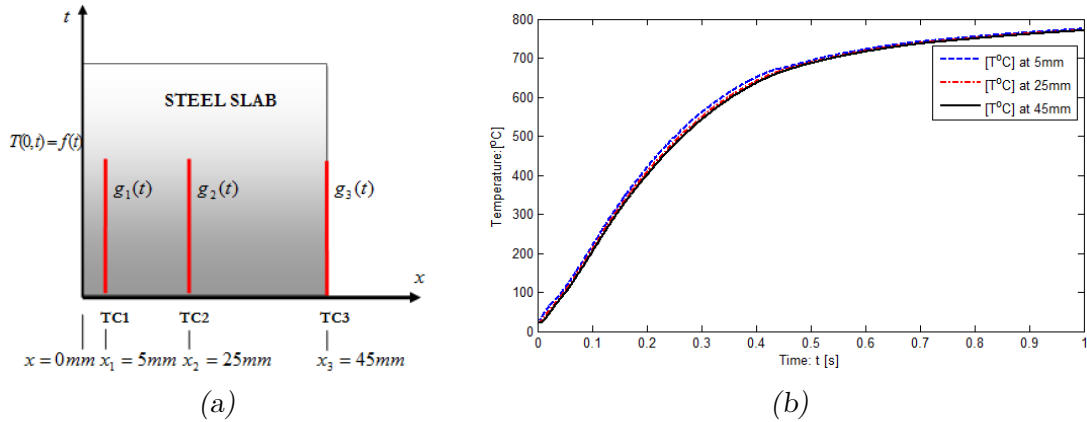


Fig. 3.3: (a) shows the positions of the thermocouples $TC1$, $TC2$, and $TC3$ inside the material. and (b) shows from the top, middle, and bottom the measured temperature histories inside the slab at position $x = 5\text{mm}$, 25mm , and 45mm , respectively as shown in Fig.3.2.

To illustrate the usefulness of the inverse method in estimation of surface temperature in real industrial application, the heat conduction equation in original problem (1.11) is rewritten

as

$$T_t(x, t) = \alpha T_{xx}(x, t), \quad \alpha = \kappa T_0 / c_p \rho L^2 \quad (3.1)$$

where α is the thermal diffusivity of the material, with T_0 is the total time for the heating experiment, and L is the distance to thermocouple from the surface, [43]. The thermal conductivity, density, and specific heat capacity of the used material are $\kappa = 30W/mK$, $\rho = 7500kg/m^3$, and $c_p = 680Ws/kgK$ respectively and also the total time for the heating experiment, $T_0 = 93.7s$. In addition, the distance between the surface at $x = 0mm$ and the thermocouple $TC1$ is $L_1 = 5mm$ and the distance between the thermocouple $TC1$ at $x = x_1$ and thermocouple $TC2$ at $x = x_2$ is $L_2 = 20mm$.

Even if, the purpose of the thesis is to estimate the surface temperature, $T(x = 0, t)$ we first test our developed method by comparing the measured and the calculated temperature histories at position $x_1 = 5mm$, where the temperature gradients at that position $x = x_2 = 25mm$, see *Fig.3.4(c)* was used to compute the heat fluxes shown in *Fig.3.4(d)* at the same location, which served as boundary data for the inverse problem and it was obtained by solving a well-posed boundary problem in the interval $[x_2, x_3]$, the results from comparison are given in *Fig.3.5(b)*.

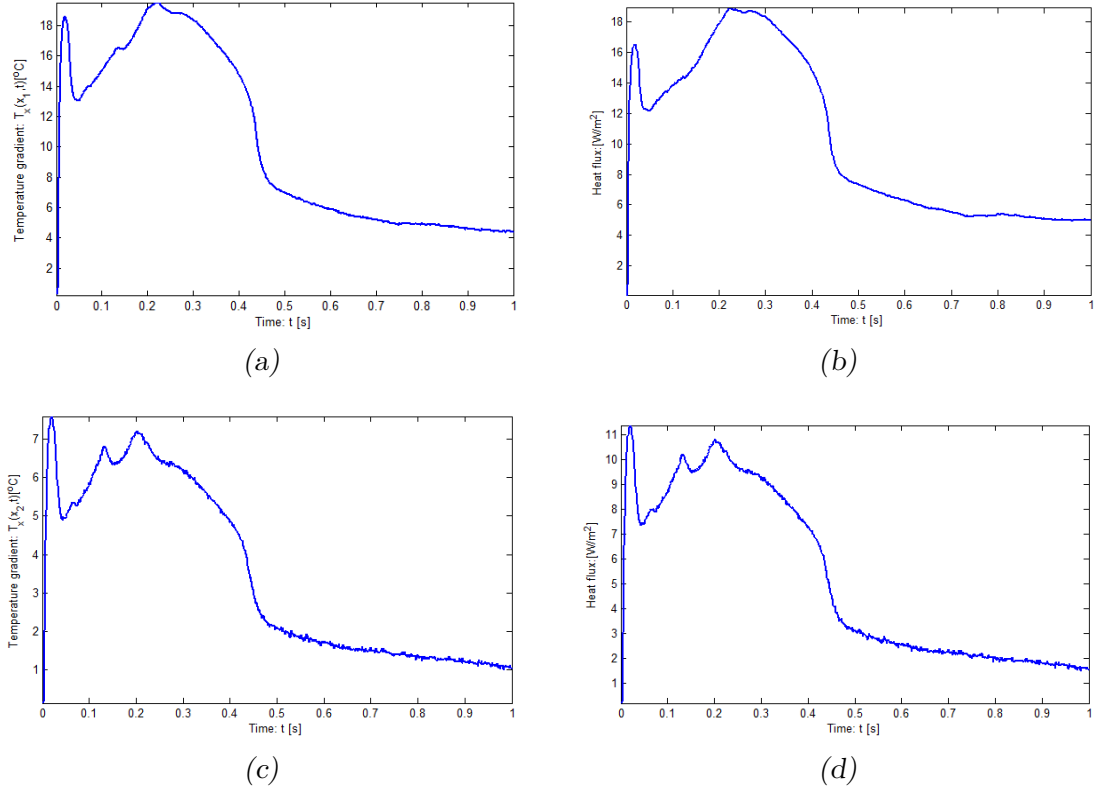


Fig. 3.4: The top left, and right subplots show respectively, the calculated temperature gradients and heat fluxes at $x_1 = 5mm$ below the surface, and the bottom left, and right subplots show respectively, the calculated temperature gradients and heat fluxes at $x_2 = 25mm$ below the surface.

Finally, to estimate the surface temperature, $T(0, t)$ of the slab; the data recorded by ther-

thermocouples at position $x = x_1$ and $x = x_2$ have been used. The temperature gradients shown in *Fig.3.4(a)* were used to calculate the heat fluxes shown in *Fig.3.4(b)* at position $x = x_1$ which have been used as boundary data for inverse problem; and also more additional data, heat fluxes at position $x = x_2$ was included so that two data vectors, i.e, heat fluxes at position $x = x_1$ and at $x = x_2$ have been used to estimate surface temperature $T(0,t)$, the results are displayed in *Fig.3.6*.

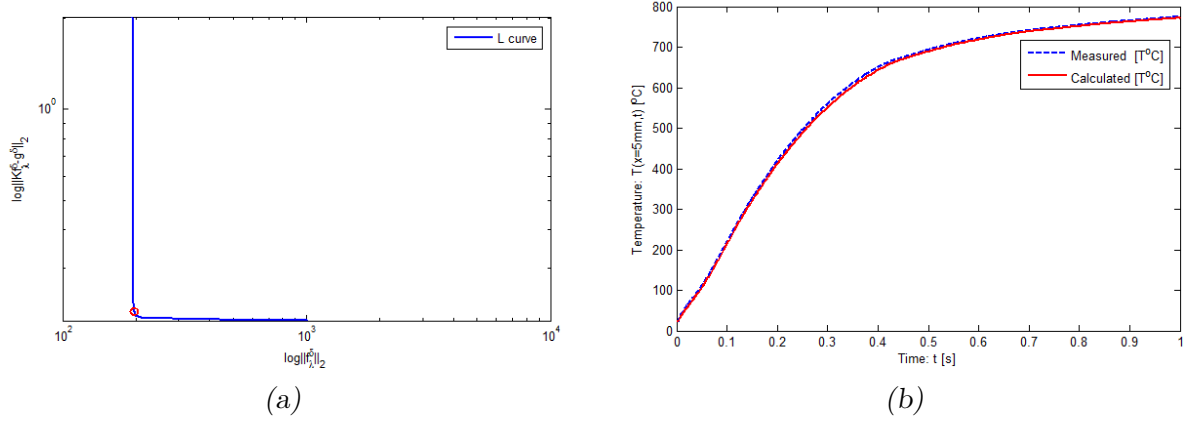
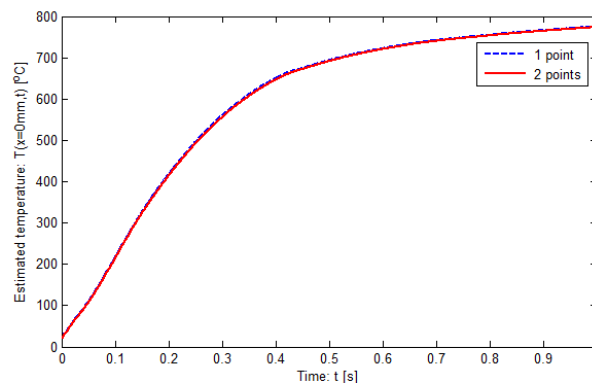


Fig. 3.5: The left subplot is the L-curve, where the regularization parameter is $\lambda = 0.0032$, and the right subplot shows the measured temperature histories (dashed-line) at $x_1 = 5\text{mm}$ below the surface of the slab and the calculated temperature (solid-line) at $x_1 = 5\text{mm}$ below the surface of the slab.

The result from the comparison of the calculated and measured temperature by thermocouple *TC1* positioned at $x_1 = 5\text{mm}$ below the surface of the slab revealed that the average difference between the measured and the calculated value is 4.9°C which is a very good result, since the temperature histories ranged between 20°C to 800°C .



*Fig. 3.6: The **dashed-line** is the estimated surface temperature, $T(0,t)$, using the measured temperature histories at one measurement point $x_1 = 5\text{mm}$ below the surface and the **solid-line** is the estimated surface temperature, $T(0,t)$, using the measured temperature histories at two measurement points, $x_1 = 5\text{mm}$ and $x_2 = 25\text{mm}$ below the surface of the slab.*

4. DISCUSSION AND CONCLUSION

The main objective of the thesis was to estimate the surface temperature of a steel slab by solving an inverse heat conduction problem. However, in application, the surface itself is inaccessible for direct measurements or locating a measurement device such as a thermocouple on the surface would disturb the measurements so that an incorrect temperature measurement is recorded. In this situation, we are restricted to interior measurements, from which we approximated the surface temperature by solving an inverse heat conduction problem in the region between the surface and a measurement point, because this process is strongly influenced by the time dependent temperature and heat-flux close to the surface.

Thus, the Crank-Nicolson implicit scheme was used to compute temperature distribution, $T(x, t)$, inside the material, by treating the discretization both in space and in time of

$$(a(x)T_x)_x = T_t, \quad x, t \in [0, 1]$$

where $a(x)$ is theoretical thermal diffusivity of the material, and the problem (2.6) was formulated as linear discrete problem (2.35), $Kf = g^\delta$ with K , f , and g^δ are matrix and vectors described in Section 2.3 and 2.5. Finally, Tikhonov regularization method given in Section 2.4.1 was implemented to recover the theoretical function $f(t)$ from numerical experiments in test problems Test 1 up to Test 5. Some results are summarized here in *Fig.4.1* below.

In addition to numerical examples given in test problems Test 1, Test 4 and Test 5, other numerical example was performed by using nine measurement points, $x = 0.1, 0.2, \dots, 0.8, 0.9$ to see the effect of using more interior measurement points and the effect of using the points far from the surface, $x = 0mm$ in estimation surface temperature, $T(0, t)$. The norm errors between the exact and the estimated solutions, $\|f - f_\lambda^\delta\|_2$ are 1.9375, 1.5752, 2.3123 and 0.5036 for the results displayed in *Fig.4.1(a)* to *Fig.4.1(d)*. From this results we see that in general the more we increase the number of measurement points in estimation of $T(0, t)$, the more we get the accurate results, the same conclusion can be made from results presented in *Fig.2.13(a)*.

However, from Test 5 where four measurement points $x = 0.8, 0.85, 0.9, 0.95$ including the point where temperature is zero, $x = 1$, the high error of 2.3123 was observed. The physical meaning of that result in heat treatment of steel is that the distance L to the measurement point closest to the surface is the most important thing to consider in heat treatment of steel, since L represents the amount of material that needed to be heated before a change in

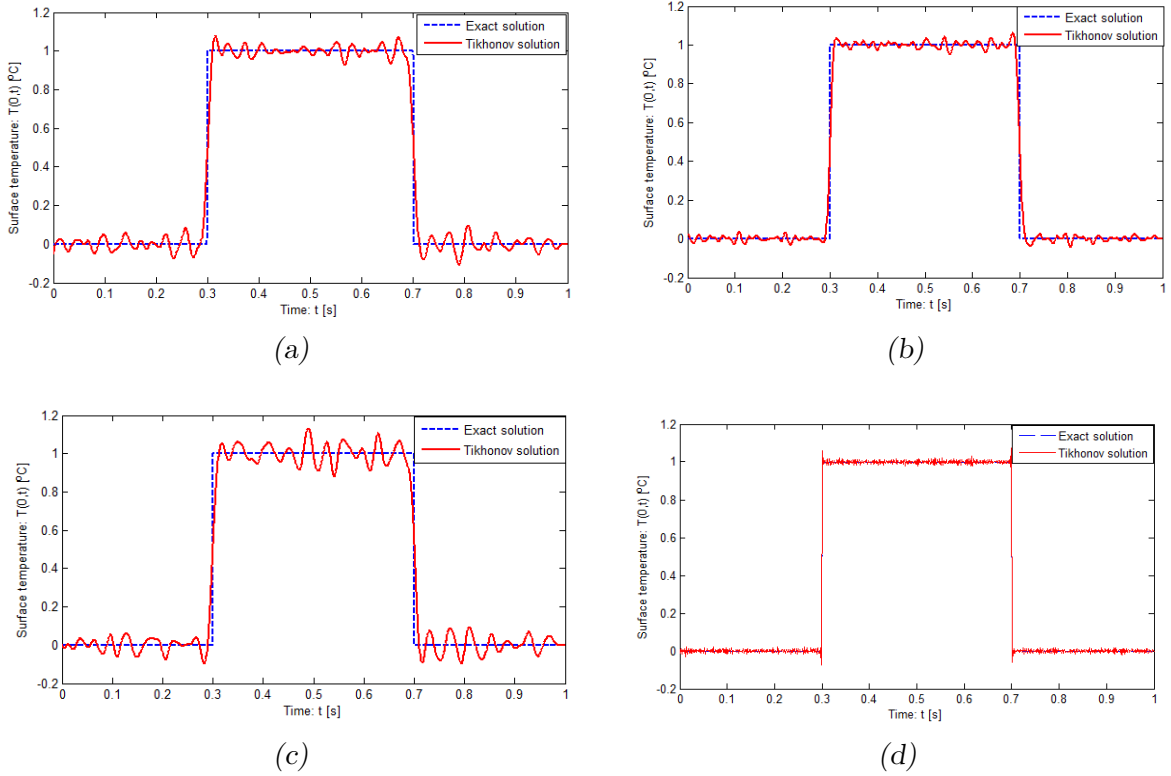


Fig. 4.1: The (a)-(c) subplots show the results from the numerical examples Test 1, Test 4 and Test 5. The subplot (d) is the results obtained by using nine measurement points.

surface temperature is seen at the thermocouple. Thus, the larger L is, the more energy is required to heat the material before the change in temperature is visible. Therefore, we can conclude that using more measurement points improve the results, but it would be better if the measurement points are closer to the surface.

Moreover, the developed method for estimation of surface temperature, $T(x = 0, t)$ was applied to a real industrial problem where the measured temperature histories inside the steel slab at three position $x_1 = 5mm$, $x_2 = 25mm$ and at $x_3 = 45mm$, were taken during an industrial steel quenching process published in [12]. In Section 3.2 the developed method was used to calculate the temperature histories at $x = 5mm$ below the surface, the result were compared with the actual measured temperature at the same location and are presented in Fig.3.5(b). Finally, $T(x = 0, t)$ was estimated using the heat fluxes calculated at $x_1 = 5mm$ and again using both heat fluxes calculated at $x_1 = 5mm$ and at $x_2 = 25mm$ as boundary data of inverse problem, the results are shown in Fig.3.6. Even though, the measurements taken inside the slab have some random noise, those random noise was dealt with the Tikhonov regularization property of the inverse method.

Therefore as conclusion, based on the results obtained from all numerical experiments presented and comparison between calculated and measured temperature from industrial application, we can conclude that the Tikhonov regularization method works well, and it

can be applied to the problems with variable coefficients. We also conclude that using more additional measurement points improved the accuracy of the solution in estimation of surface temperature as well as improving the stability of the inverse problem. Finally, we recommend that the developed method can be used in similar industrial applications where the surface itself is inaccessible for direct measurements or locating a measurement device for some reasons in steel industries.

BIBLIOGRAPHY

- [1] H.S.Carslaw. Introduction to the Mathematical Theory of the Conduction of Heat in Solids. Second edition, Macmillan and co., Limited, London, (1921).
- [2] David V.Widder. The Heat Equation. Harvard University, Academic Press, (1975).
- [3] J.Kervorkian. Partial Differential Equation: Analytical solution techniques. University of Washington, Wadsworth, Inc, (1990).
- [4] Jan Taler Piotr Duda. Solving Direct and Inverse Heat conduction Problems, Springer, (2006).
- [5] James V. Beck, Ben Blackwell and Charles R.ST. Clair, JR. Inverse Heat Conduction, Ill-Posed Problems, New York, John Wiley Sons, (1985).
- [6] Walter A.Strauss. Partial Differential Equation an Introduction. John Wiley Sons, Ltd; Second Edition. Vol.21, No.6, SIAM, (2007).
- [7] Lawrence C.Evans. Partial Differential Equations. American Mathematical Society, Second Edition, (2010).
- [8] Fredrik Berntsson. A spectral method for solving the sideways heat equation, Linköping University, S-581 83 Linköping, Sweden, (1999).
- [9] Heinz W.Engel, M.Hanake and A.Neubaur. Regularization of Inverse Problems. Kruwer Academic Publishers, London, (1996).
- [10] Charles F.Weber. Analysis and solution of the ill-posed inverse heat conduction problem. Journal of Heat Transfer, vol.24, No.11. Pergamon Press Ltd, (1981).
- [11] Muhammad Aamir, Qiang Liao, Xun Zhu, Aqeel-ur-Rehman, Hong Wang, and Muhammad Zubair. Estimation of Surface Heat Flux and Surface Temperature during Inverse Heat Conduction under Varying Spray Parameters and Sample Initial Temperature. The Scientific World Journal Volume 2014 Article ID 721620, <http://dx.doi.org/10.1155/2014/721620>, Hindawi Publishing Corporation, (2014).
- [12] Patrik Wikstrom, Wlodzimierz Blasiak and Fredrik Berntsson. Estimation of the Transient Surface Temperature, Heat Flux and Effective Heat Transfer Coefficient of a Slab in an Industrial Reheating Furnace by using an Inverse Method, Elsevier, (2007).

-
- [13] Patricia K.Lamm. Approximation of Ill-posed Volterra Problems via Predictor-Corrector Regularization Methods. Vol.56, N_0 .2, SIAM, (1996).
- [14] Patricia K.Lamm and Lars Elden. Numerical solution of Frist-kind Volterra Equations by Sequential Tikhonov Regularization. Vol.34, N_0 .4, SIAM, (1997).
- [15] Lars Elden, Fredrik Berntsson, and Teresa Reginska. Wavelet and Fourier Methods for Solving the Side Heat Equation. SIAM, (2000).
- [16] C.E.Mejia, D.A. Murio. Numerical Solution of Generalized Inverse Heat Conduction by Discrete Mollification, (1996).
- [17] O.R. Buregraf. An Exact Solution of the Inverse Problem in Heat Conduction Theory and Applications. Journal of Heat transfer, (1964).
- [18] Alexander A.Samarskii, and Peter N.Vabishchevich. Numerical Methods for solving Inverse Problems of Mathematical Physics, Walter de Gruyter GmbH and Co. KG, D-10785 Berlin, Germany, (2007).
- [19] Fredrik Berntsson. An Inverse Heat Conduction Problem and Improving Shielded Thermocouple Accuracy, Numerical Heat Transfer, Part A: Applications. An International Journal of Computation and Methodology,61:10, 754-763, (2012).
- [20] Victor Isakov. Inverse Problems for Partial differential Equations. Second edition, Springer, (2006).
- [21] Oleg M.Alifanov. Inverse Heat Transfer Problems, Springer-Verlag, (1994).
- [22] Gene H.G& Charles F.V.L. Matrix Computations Fourth Edition, (2013).
- [23] Curtis R.Vogel. Computational Method for Inverse Problems. Society for Industrial and Applied Mathematics(SIAM),Philadelphia, (2002).
- [24] Andrey.N Tikhonov& Vasily Y.Arsenin. Solutions of Ill-Posed Problems. John Wiley& sons, (1977).
- [25] Per.C Hansen. Rank-Deficient and Discrete Ill-Posed Problems. SIAM, (1998).
- [26] G.Stolz,JR. Numerical Solutions to an Inverse problem of Heat Conduction for Simple Shapes, (1960).
- [27] E.M.Sparrow, A.Haji-Sheikh, and T.S.Lundgren. The Inverse Problem in Transient Heat Conduction, (1964).
- [28] Diego A.Murio. The Mollification Method and the Numerical Solution of Ill- Posed problems, (1993).

-
- [29] Ksaku Yosida. Functional Analysis. Six Edition, Springer-Verlag, (1980).
- [30] Erwin Kreyszig. Introductory Functional Analysis with Applications. John Wiley & Sons, (1989).
- [31] Rabindranath Sen. A first Course in Functional Analysis, Theory and Applications. Anthem Press, (2013).
- [32] John D. Anderson, JR. Computational Fluid Dynamics: The basics with Applications. McGraw-Hill, (1995).
- [33] Randall J. LeVeque. Finite difference methods for ordinary and partial differential equations: Steady state and time dependent problems. Society for industrial and Applied Mathematics (SIAM), (2007).
- [34] G.D. Smith. Numerical solution of partial differential equations: finite difference methods. Oxford University Press. Third Edition, (1985).
- [35] J. Crank and P. Nicolson. A practical method for numerical evaluation of solutions of partial differential equations of the heat conduction type. Mathematical Proceedings of the Cambridge Philosophical Society, (1947).
- [36] Albrecht B. & Sergei M. Grudsky. Toeplitz Matrices, Asymptotic Linear Algebra, and Functional Analysis. Springer Basel AG, (2000).
- [37] Heinz W. Engl & Wilhelm Grever. Using L-curve for determining optimal regularization parameters. Springer-Verlag, (1994).
- [38] V.A. Morozov. Methods for Solving Incorrectly Posed Problems. Springer-Verlag New York Inc, (1984).
- [39] Per.C Hansen. Analysis of Discrete Ill-Posed Problems by means of the L-curve. SIAM, (1992)
- [40] Per.C Hansen & Dianne.P O'Leary. The Use of the L-curve in the regularization of discrete ill-posed problems. SIAM, (1993).
- [41] CR Vogel. Non-convergence of the L-curve regularization parameter selection, (1996).
- [42] Martin Hanke. Limitations of the L-curve method in ill-posed problems. BIT, (1996).
- [43] Fredrik Berntsson. Numerical Solution of an Inverse Heat Conduction Problem. ISBN 91-7219-316-6, ISSN 0280-7971. UniTryck, Linköping, (1998).